Pb AND Zn CONTAMINATION IN ZOAR VLEI, CAPE PENINSULA

By Caroline Emma Reid

BSc(Hons)

Submitted in partial fulfilment of the requirements for the degree of Master of Science,

Department of Geological Sciences, University of Cape Town.

January 1995

ABSTRACT

The sediments in Zoar Vlei act as a considerable sink for Pb and Zn derived from the adjacent Paarden-Eiland semi-industrial area and the Milnerton-Rugby residential area. Through elemental analysis of 34 sediment samples by WDXRF spectroscopy, the sediments were shown to be significantly enriched in Pb and Zn. Lead and Zn concentrations are highest at the entrance to the southern pan, and decrease northwards through the vlei system. Kaolinite, quartz, illite and smectite are present in the clay fraction of the sediment, as was shown by analysis of a clay separate by XRD. The results of the sorption experiments revealed that both Pb and Zn are sorbed by the sediments. The selective affinity of the sediments for Pb exceeds that for Zn, as Pb sorption was shown to displace Zn from the sediment, while Zn sorption did not induce Pb release. The high degree of irreversibility of both Pb and Zn sorption indicates that sorption is specific in nature, and that under the present environmental conditions, the sediments act as a suitable storage facility for these metals. Acidification of the vlei water in equilibrium with the sediments caused Zn release through neutralisation reactions. Total water analyses were performed on 72 vlei water samples using high performance ion liquid chromatography and ICP-AES. Zinc concentrations in the vlei were elevated compared to natural background values, and decrease in a northerly direction through the vlei system, however remain elevated at the outflow into the Milnerton Lagoon. Zinc appears to be entering the vlei via stormwater drains from both the industrial and residential areas. Through the use of the MINTEQA2 computer speciation programme, it was shown that the majority of the dissolved Zn is present as the $Zn(OH)_2(aq)$ species. Carbonate complexation appears to initially control Pb solubility, as a Pb carbonate precipitate was observed to form on addition of Pb to vlei water and the dissolved Pb is predominantly present as $Pb(CO_3)_2^{2-}$ and $PbCO_3(aq)$. However, concentrations of dissolved Pb in equilibrium with Pb carbonate exceed those observed in the vlei water and in the supernatants of the adsorption experiments. Thus the solubility of Pb and Zn on entering the vlei appears initially to be controlled by precipitation of Pb and Zn carbonate. However once equilibrium with the sediments is achieved, sorption reactions are more likely to exert a greater control on metal solubility.

TABLE OF CONTENTS

INTRODUCTION

The sediments in Zoar Vlei act as a considerable sink for various transition metals and other elements derived from the adjacent Paarden Eiland semi-industrial area. This has led to unusually high concentrations of Zn (max = 3830ppm), Cu (max = 200ppm), Pb (max = 472ppm) and As (max = 29ppm) (Board, 1993; Farmer, 1993). Pb and Zn particularly have been concentrated in the sediments of Zoar Vlei by anthropogenic activities. Due to the high toxicity potential of both Pb and Zn, it is necessary to investigate the permanence of the sediments as a storage facility for these metals. The mechanisms and processes by which the metals are bound to the sediment particles require identification in order to understand the mechanisms by which, and the conditions under which, metal release would occur. In short the mobility of Pb and Zn in this particular aquatic environment requires investigation.

The aims of this study are as follows:

1. To assess the areal distribution and the extent of Pb and Zn pollution in the sediments of Zoar Vlei, in order to verify the results presented by Board (1993) and Farmer (1993).
2. To determine the concentration of Pb and Zn in the vlei water in order to determine the efficiency of the sediments at removing trace metals and to determine whether elevated Pb and Zn concentrations are present in the vlei water.
3. To determine the speciation of dissolved Pb and Zn in the vlei water, as this will effect the bioavailability of these metals and their potential for adsorption. ion.
4. To identify the clay mineralogy of the sediments and interpret this information in the context of metal adsorption.
5. To explore the nature of Pb and Zn adsorption by and desorption from the sediments under different conditions of pH and salinity, in order to identify the environmental conditions under which adsorption would be severely reduced, leading to metal release from the sediments.

CHAPTER 1

Factors influencing the mobility of Pb and Zn in aquatic sediments - A review

1.1. Introduction

There is considerable evidence in the literature that contaminants are taken up and concentrated by sediments in the aquatic environment (Hart, 1982). Transportation of these contaminants in association with particulate matter represents a major pathway in the biogeochemical cycling of trace contaminants (Hart, 1982). The aquatic environment is a dynamic system consisting of diverse residents states of transition metals. The affinity of the transition metals for the various states is expressed by thermodynamic parameters such as solubility products and partition coefficients for the equilibrium state (Forstner and Wittman, 1979). It is possible to conceptualise the essential pathways for trace metals in the biogeochemical cycles of freshwater systems (Hart, 1982). Because kinetic and thermodynamic information is lacking, detailed information on the mechanisms controlling this trace metal flux is scarce and therefore accurate quantitative predictions on trace metal behaviour cannot be made (Hart, 1982).

Anthropogenically derived metals released into an ecosystem tend to accumulate in sediments through various adsorption and precipitation processes (Coetzee, 1993). In order to gain insight into the adsorbing capacities which sediments display towards metals i.e. whether a metal tends to remain solubilised or adhere to particulate material, their sequence of residence times in the aqueous phase of a given system can be compared (Table 1, Forstner and Wittman, 1979). Both Pb and Zn have relatively short residence times compared with other trace metals, indicating their strong affinity for the solid phase.

It is now widely accepted that the ecological significance of metal inputs and toxicity potential of the metals is determined by the specific form and reactivity of the metal compound in the sediment, rather than by its concentration and rate of accumulation (Forstner, 1987). The major mechanisms of accumulation of heavy metals in

sediments result in five basic metal states in sediments : 1. Adsorptive and exchangeable metal; 2. metal bound to carbonate phases; 3. metal bound to reducible phases; 4. metal bound to organic matter and sulphides; and 5. detritus and lattice metals. The experimental determination of the proportion of metal in each of the above five categories can be achieved through the use of various sequential extraction procedures (Pardo *et al.*, 1990). This information is extremely valuable in environmental pollution control monitoring as the categories of metals behave differently with respect to remobilisation under different environmental conditions (Pardo *et al.*, 1990). Metals in the interlayer positions of clays or incorporated into the crystalline structure of minerals are relatively immobile. Alternatively, metals which are available for biological uptake or for further reaction upon changes in Eh or pH include those co-precipitated with hydrous iron or manganese oxides, complexed with organic matter, adsorbed onto the surfaces of particulate matter or dissolved in the pore water (Filipek and Owen, 1978). The metal contaminants introduced into the aquatic environments by human activities usually exist in a relatively unstable chemical form, and are therefore more accessible to short and medium-term geochemical processes (Forstner, 1987). The metal content in the inert phases is of detrital and lattice origin and unavailable for release in natural environments. The proportion of easily released to inert trace metal is a reliable measure of the level of pollution of the sediment (Forstner and Wittman, 1979). The large proportion of easily released metal in the sediments of Zoar Vlei determined by Board (1993) and Farmer (1993) confirms the anthropogenic origin of the metal.

In principle the partitioning of sediment bound metals could be evaluated by both thermodynamic calculations (provided equilibrium conditions prevail) and by experimental sequential extraction techniques (Rapin *et al.*, 1986). The application of thermodynamic data to real systems is limited due to the complex nature of real sediments, thus the latter method is most often employed when investigating real situations (Hart, 1982).

The use of sequential extraction procedures is not without criticism. Doubt has been cast on the validity of the results obtained by such techniques, mainly due to two

possible sources of error. Firstly, the chemical extractant may attack phases other than those expected, and, secondly, once the metals are liberated from one phase they may become associated with another rather than staying in solution (Hart, 1982). Rapin *et al.* (1986) report the numerous factors which influence such extraction procedures, such as the choice of reagents used, the sequence of extraction, the time of extraction, the ratio of extractant to sediment and the numerous inherent analytical problems such as incomplete selectivity and re-adsorption. It therefore follows that the distribution of a metal among various extractable fractions does not necessarily reflect its association with the sedimentary phases, but rather should be operationally defined by the method of extraction. The most often used sequential extraction technique used is that derived by Tessier *et al.* (1979), which involves the use of leaching agents of different strengths to selectively extract out trace metals associated with different geochemical phases due to different complexation strengths (Hart, 1982).

An understanding of the processes by which the metals are bound to the solid phase is crucial to the ability to predict the conditions that would lead to their release. The solubility of heavy metals is rarely controlled by equilibrium with sparingly soluble solids, but rather related to sorption and co-precipitation phenomena (Karlsson *et al.*, 1988). The specific adsorption mechanism is not always evident under field conditions as it is difficult to define the nature of the solid surface at which adsorption is occurring (Hart, 1982). Thus research on sorption mechanisms has focused on laboratory experiments involving pure well defined surfaces such as clays, Al_2O_3, FeOOH and MnO_2. The limitations of these results lie chiefly in the difficulties encountered in extrapolating the results from these model studies to natural sediments, as there is usually a general neglect of other possible influences in the experimental design, such as competing ligands in the aqueous phase (Hart, 1982).

1.2. Adsorption of Pb and Zn

1.2.1. Clay surfaces

Interest in the adsorptive properties of clay minerals has increased greatly in recent years. However, much still remains to be learned about the adsorption processes and

relative affinities of clay minerals for trace metals (Farrah *et al.*, 1980). Adsorption can arise from the electrostatic attraction between metal and negatively charged surface site alone, in which case adsorption is relatively non-specific and non-selective. Alternatively, the electrostatic attraction may be augmented by hydrogen bonding, coordinate bonding or Van de Waals bonding (Forstner and Wittman, 1979). Non-selective adsorption involves the exchange of cations between the negatively charged surface and the aqueous solution. The cation exchange capacity of clay minerals is governed by their structure and increases in the following order: kaolinite < chlorite < illite < montmorollonite. The large cation exchange capacity of montmorollonite is a function of its characteristically large interlayer distances and accompanied swelling. The sequence of increasing cation exchange capacities of the common clay minerals is also related to the reduction in average particle size and the corresponding increase in surface area. Forstner and Wittman (1979) report that the affinities of the cations towards exchangers is governed by the following factors :

1. Valence and hydration effects - the affinity increases with increasing oxidation number and decreasing diameter of the hydrated cations.
2. The concentration of the solution - an increase in the concentration of exchangeable cations will increase the number of cations exchanged (complying with le Chateliers Principle); negatively charged surfaces in equilibrium with cations of different valencies show preference for species with higher charge densities.
3. Reactions involving hydrolysed cations - experimental evidence indicates that heavy metal hydroxy species are adsorbed in preference to the uncomplexed cation (Forstner and Wittman, 1979). Evidence supporting this theory is that the pH at which maximum adsorption occurs is closely correlated with the pH marking the onset of hydrolysis of the metal cation (Jean and Bancroft, 1986).
4. Specific reactions between clay surfaces and the cations.

Forstner and Wittman (1979) report that the selective affinity of trace metals towards clay surfaces increases in the following sequence: Pb < Cu < Zn. This is determined by plotting a graph of dq vs U where q is the concentration of the cation adsorbed and U is equal to the amount of cation feeding per 100g of adsorbent. Thus dq/dU

vs U is a means of expressing the competitive adsorption power of each cation where a negative dq/dU indicates desorption. Such a plot illustrates that at the beginning of the adsorption process there are sufficient available sites on the mineral surface to facilitate the equal adsorption of all metals. As the number of adsorption sites becomes limited, adsorbed Cu and Zn are displaced by Pb (Forstner and Wittman, 1979). This result is highly dependant on the type of adsorbent and the pH, Eh and salinity of the liquid phase which will influence the speciation of the metals in solution, and therefore the relative amount of adsorption of each metal. The exchange of cations on a mineral surface can be expressed by the following equation:

M_1, clay + M_2 = M_2, clay + M_1 (Farrah et al., 1980).

The slope of the exchange plots (i.e.$(M_1/M_2)_{aqueous}$ vs $(M_1/M_2)_{clay}$) is termed the selectivity coefficient and defines the relative affinity of the clay surface for cations M_1 and M_2 at equilibrium. However, exchange plots tend to form waves rather than lines indicating reversals in selectivity values. This is a function of the heterogeneous nature of the clay surfaces. The clay surfaces possess several different sites each having a different affinity for different ions (Farrah *et al.*, 1986). For example, with clay suspensions both interlayer and surface sites exist, and should these differ with respect to geometry and chemical nature then certain cations will be held more tightly than others. Further evidence for this heterogeneity of sites is the fact that trace metal desorption into extraction solutions has been found to be incomplete, even at extractant concentrations that should displace all the physically adsorbed metal (Di Toro *et al.*, 1986). This incomplete desorption is partly the result of the creation of new adsorption sites through the adsorption of silicate ions (Farrah *et al.*, 1980).

The relationship between equilibrium solution concentrations and the concentration of the species adsorbed can be described by a Langmuir isotherm, the slope of which at a particular equilibrium concentration is equal to the partition coefficient K_D (Farrah *et al.*, 1980). At small sorption densities all types of sites are available in excess, whereas at higher sorption densities the availability of the strongest binding sites is limited, which leads to a decrease in the apparent adsorption equilibrium constant (Houba *et al.*, 1983). Farrah *et al.* (1980) present experimentally determined

adsorption isotherms for adsorption of Mg, Cu, Cd, Pb and Zn onto Na^+ form montmorillonite, illite and kaolin. The slope and shape of the experimentally determined adsorption isotherms vary with the nature of the adsorbate and the adsorbent. If the adsorption mechanism was a simple stoichiometric ion exchange process, then the slope and the shape of the Langmuir isotherm would be reasonably independent of the cation used. From the observed differences in behaviour one can only conclude that not all sites are accessible to each cation to the same extent (Farrah *et al.*, 1980). Thus reversal of the selectivity coefficients occurs at the intersection of the isotherms for the different cations.

1.2.2. Sulphide mineral surfaces

Jean and Bancroft (1986) investigated the adsorption of aqueous Hg, Pb, Zn and Cd complexes on a variety of sulphide minerals as a function of solution pH and the nature of the ligands in solution. They concluded that sulphide minerals are excellent scavengers of trace metals and adsorption is highly pH dependant. Results of the speciation of Zn and Pb in Zoar Vlei obtained by Board (1993) and Farmer (1993) indicate that a considerable amount of Pb (max = 51%) and to a lesser extent Zn (max = 17%) is bound to organic matter and sulphidic phases. The sediments in Zoar Vlei contain abundant Fe and Mn sulphides, thus the investigation of heavy metal adsorption onto sulphide mineral surfaces is particularly appropriate to this study.

The experimentally determined pH dependence of adsorption of Zn and Pb onto sulphide mineral surfaces, as well as the speciation of the metal in solution at a given pH without the presence of the sulphide, is presented by Jean and Bancroft, (1986). For each solution there is a critical pH range or adsorption edge at which the adsorption increases dramatically. Jean and Bancroft (1986) define the pH at which 50 % of the initial metal is adsorbed as pH_{50}. The pH_{50} for Pb and Zn adsorption is 6.5 and 6.7 respectively. At pHs of < 7, Pb is predominantly present as the $Pb(NO_3)^+$ species and the free divalent cation. Above neutral pHs the $Pb(OH)^+$, $Pb(OH)_2$ and $Pb(OH)_3^-$ species dominate, their abundance peaking at pH 8.5, 11 and 14 respectively. Jean and Bancroft (1986) report that at a Ph of approximately 8.5 Zn

is present in solution as the free divalent zinc ion. At a pH exceeding 8.5 the $Zn(OH)_2$ species predominates. It is evident that the pH dependence of adsorption for a particular metal varies with metal concentration and the nature of the adsorbent. This indicates that it is the speciation of the metal in the aqueous solution (which is pH dependant) that controls adsorption. It is believed by many workers (Jean and Bancroft, 1986; Forstner, 1987; Salomons *et al.*, 1987) that the position of the adsorption edge is related to the ease of hydrolysis and preferential adsorption of the hydrolysed species.

Co-precipitation of Pb and Zn sulphide minerals with the Fe sulphides is probable in a sulphide-rich reducing environment, as heavy metal sulphides are highly insoluble. There is no apparent difference between chemisorption and co-precipitation. Experiments on Cd adsorption and co-precipitation with amorphous iron oxyhydrate have shown that the removal efficiency of the Cd is identical whether the iron is precipitated before the trace metal is added (adsorption) or afterwards (co-precipitation) (Forstner, 1987). Precipitation requires that the solubility product is exceeded. The solubility product for both PbS and ZnS is extremely low. Thus under highly sulphidic conditions the required concentration of Pb and Zn in the aqueous solution for the precipitation of the various metal sulphides is easily achieved (Forstner and Wittman, 1979). Precipitation of PbS and ZnS would continue until insufficient Pb and Zn are present in the aqueous solution to fulfil the stoichiometric requirements of the metal sulphide minerals. In the strongly anoxic sediments of the mud flat in the Scheldt estuary, Belgium, Cd and Pb are reported to be trapped as poorly soluble metal complexes, and the metals only become available to organic matter in the suboxic and oxic environments (Panutrakul and Baeyens, 1991).

1.2.3. Organic materials

The importance of solid organic matter as an adsorbent for trace metal cations is not adequately known. However, it is believed that the trace metal adsorption capacity of organic matter is between that of clays and metal oxides (Hart, 1982). The adsorption capacity of organic matter depends on its structure, and therefore studies

on the mechanisms of organic matter trace metal interactions will only provide useful information in those instances where the humic material is well characterised (Hart, 1982). Sequential extraction techniques and various statistical tools can be used to assess the importance of organic matter complexing in real sediments. Dissolved organic matter in surface waters constitutes a major sink for trace metals by competing with solid surface ligands for metal complexation (Salomons *et al.*, 1987). However, in reduced pore waters the role of dissolved organic matter is thought to be almost negligible, as it is believed that organic matter does not complex with metals in the presence of sulphides. This is due to the fact that calculated K_D values for organic matter-trace metal complexation are much lower than equilibrium constants for adsorption and co-precipitation of sulphide phases (Salomons *et al.*, 1987).

1.2.4. Mn and Fe oxides

Fe and Mn oxides and hydroxides are normally moderately abundant in aquatic environments, and show phase transformations across redox boundaries with the oxide form of these metals existing as insoluble oxides and the reduced form as mobile ions. The high adsorption capacity of hydrous Mn and Fe oxides for trace metals suggests that these phases may control the distribution of certain trace metals in the environment (Balistrieri *et al.*, 1992). Balistrieri and Murray (1986) showed by experimentation with sediments from the Panama Basin that an increase in the solid Mn content of the sediments enhances their ability to bind Zn, Pb, Co, Cd and Ba.

Metal oxide surfaces are covered with surface hydroxyl groups in the presence of water. Thus the specific adsorption of cations can be treated as reactions with surface bound hydroxyl groups at the water - oxide interface. Adsorption in general is considered to be analogous to the formation of soluble complexes, with the surface sites thought of as ligands and their binding ability dependant on formation constants, concentration of the reacting species and other conditions such as pH_s ionic strength and competing ions (Hart, 1982).

The redox state of aquatic sediments after deposition is governed by microbiologically

mediated reactions and the utilisation of a predictable sequence of oxidants. Those affecting the main metal carriers (particularly oxides, organic matter and sulphides) and therefor the mobility of trace metals are the oxidation of organic matter and the reduction of sulphate, iron and manganese (Salomons *et al.*, 1987). Salomons *et al.* (1987) consider Fe and Mn oxides/hydroxides most important for the transport of Zn and Cd, and organic matter for the transport of Cu and in some cases Pb. The reduced forms of Fe and Mn tend to be soluble and mobile unless the ion activity products for Fe and Mn suphides, carbonates or phosphates is exceeded (Balistrieri *et al.*, 1991). In the marine environment there is a continuous supply of sulphate to the sediments and all reducible Fe is transformed into Fe sulphides. In the fresh water environment the concentration of sulphate limits Fe sulphide formation resulting in only partial transformation of Fe hydroxides to Fe sulphides. The remaining reduced Fe is precipitated as siderite given sufficient carbonate species (Salomons *et al.*, 1987). The co-precipitation of heavy metals with calcium carbonate was determined to be a large sink in the Rhine (Houba *et al.*, 1983). The availability of sulphate and reducible Fe in the system will influence the Ph which is an important variable for the solubility of trace metals (Salomons *et al.*, 1987). Numerous studies have been carried out on the cycling of Fe and Mn in lakes (Balistrieri *et al.*, 1992; Young and Harvey, 1992; Salomons *et al.*, 1987; Stauffer, 1986) as transformations of Fe and Mn across redox boundaries between dissolved and particulate phases, and the probable precipitation of FeS in the bottom waters of lakes during the anoxic period, have the potential to influence the behaviour of other trace elements through adsorption, co-precipitation and reductive dissolution processes (Balistrieri *et al.*, 1987). This process, accompanied by the degradation of organic matter and the production of hydrogen sulphide and high alkalinity, makes the formation of metal sulphides possible (Salomons *et al.*, 1987).

It is important to know whether metal concentrations in the pore waters are controlled by precipitation-dissolution reactions or by adsorption processes. There is considerable evidence in the literature favouring the presence of solid metal sulphides in anoxic sediments. This conclusion is based on the differences between the theoretical calculated solubility products for the formation of metal sulphides and

the partition coefficients governing adsorption processes (Salomons *et al.*, 1987).

The low metal concentrations in pore water dictates that the upward metal flux due to molecular diffusion will be low and will be achieved mainly due to physical processes such as consolidation and bioturbation of the sediments. When the redox barrier is intercepted Fe and Mn oxide/hydroxide precipitation will occur and the dramatic increase in adsorption sites will result in the newly precipitated material acting as a sponge and effectively cleansing the water of trace metals. Thus it may act as a chemical barrier against upward moving metal species (Salomons *et al.*, 1987).

In natural systems redox-induced changes in the distribution of trace metals merely result in the cycling of trace metals in the system. However, where redox changes that lead to the release of trace metals are anthropogenically induced problems could occur. The change from reducing to oxic conditions is of major environmental concern in land disposal of contaminated sediments, disposal in marine environments and extensive dredging of channels and waterways which leads to the resuspension of large quantities of sediment (Salomons *et al.*, 1987). Most dredged material removed and disposed of on land is high in organic matter content and clay and the microbiologically mediated decomposition reactions favour the immobilisation of contaminants provided that the dredged materials are not subject to aeration through mixing, resuspension or drying (Forstner, 1987).

1.3 Factors effecting the mobility of Pb and Zn

1.3.1. pH

The solubility, mobility and bioavailability of sediment bound metals can be increased by four major factors: 1. lowering of the pH; 2. changing of redox conditions; 3. formation of organic complexes; and 4. increasing the salinity (Forstner, 1987). Forstner 1987) reported that on a regional scale acid precipitation is probably the most important single factor affecting metal mobility in surface waters. A decrease in the pH of the liquid phase will lead to the release of adsorbed trace metals for a number of reasons:

1. The H^+ ions compete with trace metal cations for exchange sites thereby artificially releasing the latter (Forstner and Wittman, 1979). The trace metal cations can be almost completely released under extremely acidic conditions.
2. Ions released by clays in acid solutions like Ca^{+2} and Mg^{+2} also compete with the trace metals for adsorption sites (Farrah *et al.*, 1980)
3. The pH of the solution influences the speciation of the adsorbate (Farrah *et al.*, 1980).
4. Dissolution of metal carriers, particularly Fe and Mn oxides and hydroxides at low pHs, leads to the release of adsorbed trace metals (Young and Harvey, 1992).

Adsorption of metals on particulate surfaces increases exponentially from near zero to close to 100 % through a pH range of 1-2 units, and therefore a small shift in the pH of surface waters causes a sharp increase or decrease in surface metal concentrations. The onset of adsorption or the pH edge is characteristic for each metal and depends on the nature of the adsorbent and the relative concentrations of adsorbate to adsorbent. This is due to the fact that there exists a range of different site binding intensities. Thus the pH edge is not a unique function of the metal and adsorbing surface, but also depends on the solid/solution ratio (Forstner, 1987). Arafat and Jerome (1986) observed the release of trace metals from contaminated Canadian lake sediments to increase exponentially below a pH of approximately 4.0 for most trace metals. The only means of assessing the pH dependence of adsorption of trace metals onto various particulate surfaces in real systems is to perform laboratory acid leaching experiments on those sediments.

1.3.2. Salinity and the presence of organic chelators

An increase in the salinity and the concentration of organic chelators in the liquid phase will affect the mobility of trace metals in surface waters by similar mechanisms. An increase in the salinity increases the number of competing complexing ions in the water. The increase in the concentration of Ca and Mg ions influences the sorption of trace metal ions on surfaces, firstly because they are usually present in concentrations many orders of magnitude greater than trace metals, and therefor

occupy most of the surface binding sites even though they form less stable surface complexes (Millward and Moore, 1982). Secondly the calcium and magnesium ion concentrations may have a significant effect on the amount of natural organics sorbed onto particle surfaces (Hart, 1991).

An increase in the chloride ion concentration associated with an increase in the salinity may cause metal release and chloride complexation (especially with Cd) and therefore inhibit adsorption (Forstner, 1987). Frenet (1981) found that the fixation of Pb and Cd by sediment particles decreased from 96 and 90 % to 88 and 70.8 %, respectively, corresponding to an increase in salinity from 0 to 35 parts per thousand Na. They attributed this to saturation of the clays by Na^+ ions. Millward and Moore (1982) found that the pH marking the onset of adsorption of Zn onto iron oxyhydroxide varies from approximately 4.0 to 6.0 as the salinity increases from 0 to 10 parts per thousand. This observation was attributed to the formation, under acid conditions, of stable soluble mono-chloro complexes, which hinder metal adsorption. The onset of pH adsorption is also expected to shift to higher pH values with increasing chloride ion concentrations (Millward and Moore, 1982). The extent of adsorption depends to a large extent on the surface area of particulate material that is in equilibrium with the liquid. This was demonstrated by Salim (1983) who observed a significant decrease in trace metal adsorption onto aquatic sediments corresponding to an increase in the centrifugation time period of the samples. Because an increase in salinity causes clay flocculation, increasing the salinity will decrease the surface in contact with the liquid phase and therefore limit adsorption (Sinex and Helz, 1982).

The addition of organic chelators to the liquid phase has the effect of complexing the trace metals in the liquid and preventing adsorption onto particulate surfaces. Significant remobilisation of heavy metals has been observed as a result of increasing concentrations of synthetic chelators (eg nitrilotriacetic acid, NTA) (Forstner, 1987).

1.3.3. The presence of carbonate

Lead and zinc carbonate are sparingly soluble solids. Under Ph and Eh conditions prevalent in most natural systems, given the system is in equilibrium with atmospheric

CO_2, precipitation of $PbCO_3$ and $ZnCO_3$ is likely to occur, and therefor control the amount of dissolved Pb and Zn available for other processes such as adsorption (Stumm and Morgan, 1970).

1.4 Conclusions

The mobility of Pb and Zn in aquatic sediments is controlled by their strong tendency to accumulate in sediments through various adsorption and precipitation processes (Coetzee, 1993). A knowledge of the specific form and reactivity of the metal form present in the sediment is essential in order to assessthe ecological significance and toxicity potential of the metal, and to determine the processes that would lead to metal release (Forstner, 1987). This knowledge is obtained through the use of sequential extraction techniques (Rapin *et al.*, 1986). Karlsson *et al.* (1988) state that the solubility of heavy metals is rarely controlled by equilibrium with sparingly soluble solids, but rather related to sorption and co-precipitation phenomena. Clay minerals, sulphide minerals, organic matter and Fe and Mn oxides appear to be the most common substrates onto which adsorption occurs. Adsorption of metals by clay surfaces can be described by a Langmuir isotherm, the shape and slope of which is dependent on the nature of the adsorbent and adsorbate (Farrah *et al.*, 1980) and the adsorption capacity of clay minerals is governed by their structure and increases in the following order: kaolinite < chlorite < illite < montmorollonite (Forstner and Wittman, 1979). Sulphide minerals are excellent scavengers of trace metals and adsorption is highly pH dependent. pH_{50} for Pb and Zn adsorption onto sulphide minerals surfaces is 6.5 and 6.7 respectively (Jean and Bancroft, 1986). The trace metal adsorbing capacity of organic matter is generally believed to be intermediate between that of clays and oxides (Hart, 1982). Fe and Mn oxides and hydroxides have a high adsorption capacity for trace metals, and thus the distribution of trace metals in the aquatic environment may be controlled by the presence of the redox boundary. The most important factors affecting the mobility of trace metals in aquatic environments are the pH, Eh and salinity of the system, as well as the presence of carbonate and phosphate.

CHAPTER 2

Description of the study area

Zoar Vlei is situated near Milnerton in the Cape Peninsula, sandwhiched between the Paarden-Eiland semi-industrial area to the north-west and the Rugby-Milnerton residential area to the south-east (see map 1). It consists of a narrow vegetation-choked channel approximately 2 metres deep commencing in the south-west at a point adjacent to the canalised Salt River. It flows in a north-easterly direction, broadening sequentially into two elliptical, shallow flat-bottomed pans; prior to flowing into the Milnerton Lagoon via a 900mm diameter pipe that runs under the R27 and Boundary Road interchange in Milnerton (Board, 1993). Zoar Vlei represents a remnant part of the Diep River which flowed into the Salt River and then into Table Bay prior to the opening of the Diep River mouth into Milnerton Lagoon and the subsequent canalization of the Salt River in 1955 (Board, 1993). The vlei is now fed solely by run-off and storm water drains from the surrounding areas.

Situated in the Western Cape, the climate is temperate Mediterranean, characterised by winter rainfall and relatively dry summer months. Maximum and minimum daily temperatures are 26°C and 16°C, respectively, during summer and 18°C and 9°C, respectively, during winter (National Geographic Society, 1981). The highest and lowest monthly average temperatures recorded at the D.F. Malan weather station are 20.5°C for January and 12.2°C for July respectively. Annual rainfall measured at the D.F. Malan weather station is 569.6 mm, 59.2 mm falling between November and February, and 351.8 mm between May and July. In summer and winter the average number of days with rain are 3 and 9, respectively (National Geographic Society, 1981). The channels in Zoar Vlei reach a maximum depth of 2.5 metres in winter, and the pans a depth not exceeding 1.5 metres. In summer the pans and the interconnecting channel are almost dry, the only water remaining in concentrated evaporation ponds. The channel to the south-west of the southern pan and that to the north-east of the northern pan remain relatively full with a water depth of approximately 2 metres.

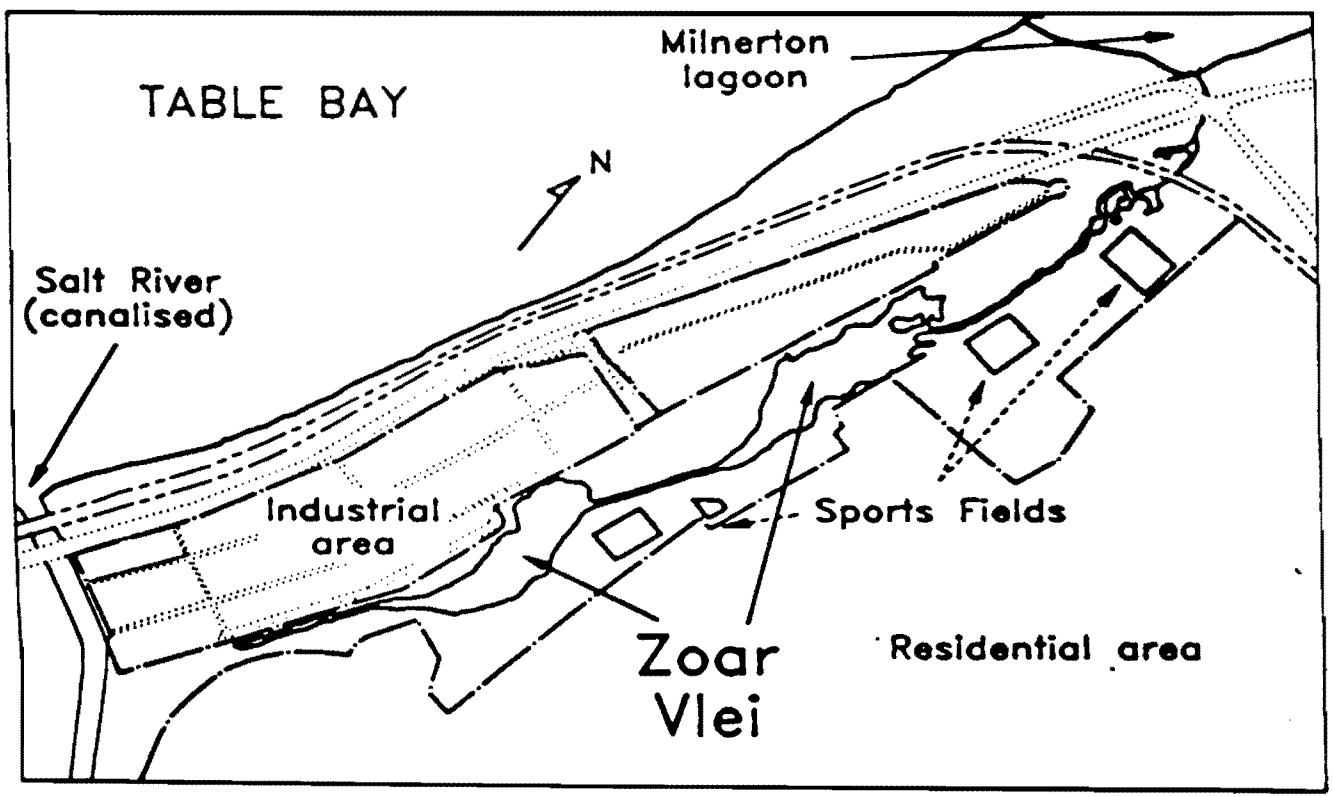

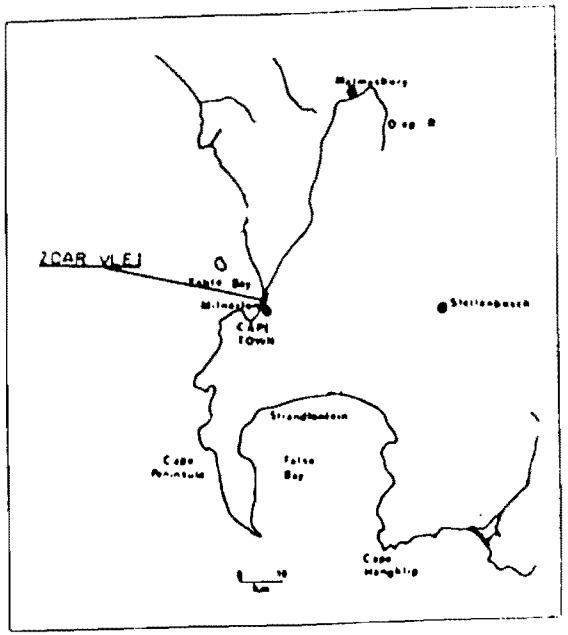

Map 1. Location of Zoar Vlei in the Cape Peninsula. Adapted from Figures 1 and 2 in Board (1993).

Zoar Vlei is situated on the Pleistocene Langebaan Formation and the Recent Witzand Formation of the Sandveld Group which are more abundantly exposed on the Cape Flats. The Langebaan Fm consists of cross-bedded, semi-consolidated aeolianites, characteristically bearing a resistant, calcretised upper surface. This is overlain by the unconsolidated, often partially vegetated, calcareous dunes of the Witzand Fm. Inland of Zoar Vlei and constituting much of the catchment area lies the Pleistocene Springfontyn Fm which is chiefly fine to medium aeolianitic quartzose sand. All the above formations are porous and permeable therefore have good aquifer properties. The Springfontyn Fm is exploited as an aquifer further north, where the town Atlantis derives all its water requirements from groundwater. The lithostratigraphy of the Cape Peninsula is shown in Table 2.1.

The sediments in Zoar Vlei are highly variable. However, Board (1993) proposed a general stratigraphic sequence from observation. The upper sediments at the sediment/water interface are fine-grained muds, up to 20cm thick in places, containing abundant organic matter and Fe and Mn sulphides. This overlays a brown to blue-grey horizon of clays and clayey sands, poorer in organic matter, and richer in sandy and shelly material than the overlying sediments (Board, 1993). Board (1993) suggests that this quite abrupt change in sedimentary facies with depth represents a change in the energy of the system; from the higher energy of the Diep River system prior to isolation, to the low energy vlei environment. The sand content of the sediments increases towards the north-east of the vlei system due to the fact that the northern pan is more susceptible to seasonal drying (Board, 1993). The sediments exhibit a high swelling capacity, those exposed prior to the rains showed very well-developed shrink-swell cracks. Expansion of the sediments occurred on re-submergence. A thin layer of a white salt or precipitate was observed on the surface of the exposed sediments.

The area directly adjacent to Zoar Vlei is artificially grassed with *Cynodon dactylon* (kweek gras). Both *Cyperus esculentis* (nut grass) and *Phragmites australis* grow abundantly adjacent to the channel banks and surrounding both pans. The channels tend to be choked by parrots feather and unidentified red algal species. The vlei

supports a large bird population, migrant waders being particularly common.

Table 2.1: Cape Peninsula lithostratigraphy (Hartnady and Rogers, 1990).

Sandveld Group	Witzand Fm Langebaan Fm Velddrif Fm Springfontyn Fm Varswater Fm Elandsfontyn Fm	Recent Pleistocene Pleistocene Pleistocene Pliocene Miocene
False Bay Dolerites		Jur-Cretaceous
Table Mountain Group	Pakhuis Fm Peninsula Fm Graafwater Fm	Silurian Silurian Ordovician
	Cape Point Intrusive	Pre-camb-Camb
Cape Granite Suite	Cape Peninsula Batholith	Pre-camb-Camb
Malmesbury Group	Sea Point Formation Bloubergstrand Fm	Late Proterozoic Late Proterozoic

Fm = Formation; Jur = Jurassic; Pre-camb = Pre-cambrian; Camb = Cambrian

Zoar Vlei is situated in the heavily populated metropolitan greater Cape Town area. The Rugby area to the south-west of the vlei is a low income residential area. The Paarden-Eiland semi-industrial area to the north-east, supports a wide variety of industries which collectively produce the following products: paint, glass, silkscreens, various electrical products, plastics, chemicals, cement, printing, machinery, furniture and photographic equipment (Board, 1993 amended by observation). The area directly adjacent to the vlei is predominantly utilised as container depots and cold storage facilities.

CHAPTER 3
Sediment composition and sorption properties

3.1. Introduction

Board (1993) and Farmer (1993) reported that anthropogenic trace metal pollution in Zoar Vlei from the adjacent Paarden Eiland semi-industrial area has led to considerable enrichment of Pb (max. conc. 472ppm) and Zn (max. conc. 3830ppm) in the sediments. The speciation of the trace metals was investigated by Board (1993) and Farmer (1993) using the sequential extraction procedure of Tessier *et al.* (1979). These results are reported in Appendix 13 and indicate that Pb is predominantly associated with the oxide and organic matter/sulphide fractions of the sediment, while Zn is mostly bound to Fe and Mn oxides (Board, 1993; Farmer, 1993).

Further sediment trace metal analyses are presented and discussed in terms of their spatial distribution and their correlation with the amount of organic carbon in the sediment in order to determine what controls the distribution of trace metals in the vlei. Karlsson *et al.* (1988) report that the solubility of trace metals is most often controlled by adsorption processes rather than by precipitation with sparingly soluble solids. One objective of this study is to investigate Pb and Zn adsorption in terms of its control on trace metal solubility.

A change in the salinity of the liquid phases may influence adsorption via two processes: Millward and Moore (1982) report that the adsorption of Zn and Pb onto iron oxyhydroxide is dependent on the salinity; an increase in salinity induces a shift of the onset of adsorption to higher pH's. A tentative suggestion is made that this hindering of adsorption is due to changes in the metal speciation with salinity; the formation of chloro-complexes as opposed to the most readily adsorbed non-hydrolysed M^{2+} ion. An increase in the salinity increases the number of ions in solution competing for adsorption sites and thus hinders adsorption of trace metals and may induce trace metal release via ion exchange reactions. Thus an objective of this study is to investigate the influence of salinity on Pb and Zn adsorption and desorption and to assess the potential for Pb and Zn release as a result of sea water

incursion into Zoar Vlei from the Milnerton Lagoon.

The increased solubility of trace metals at low pH is well documented and is due to the following factors:

- increased concentration of H^+ ions in solution which actively compete for surface sites thus changing the surface charge on adsorption surfaces (Dixon, 1989).
- the influence of pH on dissolved metal speciation (Sposito, 1989).
- the dissolution of metal carriers or adsorption surfaces at low pH (Loch *et al.*, 1991).

Acidity-induced desorption is investigated in this study for two reasons. Firstly to investigate the effects of acidification on the trace metal speciation in Zoar Vlei, as acidification could ocurr by acid ingression into the vlei system from point and diffuse sources, or through oxidation of the abundant sulphides and the resultant formation of sulphates and sulphuric acid. Secondly, from a more theoretical standpoint, because the manner in which Pb and Zn adsorption are affected by changes in pH provide information regarding the nature of the processes whereby the adsorbed metal is bound to the substrate.

3.2 Materials and methods

3.2.1 Sampling

Thirty four sediment samples were collected from Zoar Vlei in early autumn, prior to the winter rains, the locality of which are shown in map 2. Surface samples were taken using a shovel and clean plastic sampling bags, as previous studies on transition metal pollution of the sediments in the vlei (Board, 1993; Farmer, 1993) revealed the upper-most layer of the sediment to be the most heavily polluted. Sample points were chosen so as to cover the entire region, but also to focus on those areas found to be highly contaminated by Board (1993) and Farmer (1993). The samples allocated a suffix A represent the fine-grained, clay-rich top layer of sediment, while those given the suffix B represent the layer of sandier sediment beneath this. The samples were laid out on plastic sheets and sun-dried prior to being passed through a 2mm

MAP 2.

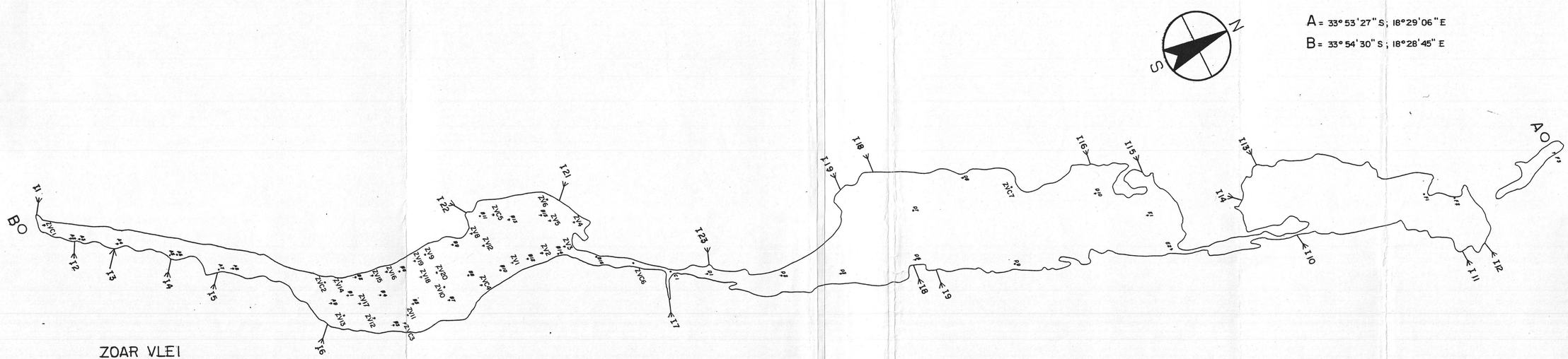

ZOAR VLEI

0 SCALE 100m

KEY:

I1 – I22 = INPUT PIPES

A2 – F3 = SAMPLE POINTS FROM BOARD (1993)

ZVC1 – ZVC7 = SAMPLE POINTS

ZV1 – ZV20 = SAMPLE POINTS

sieve to ensure a measure of uniformity of the sediment samples, and to increase the reproducibility of results.

3.2.2 Analyses and experiments

3.2.2.1 Sediment analysis

The 34 sediment samples were analyzed for Pb, Cu and Zn by wavelength dispersive X-ray fluorescence spectrometry (WDXRFS). The dried sediment samples were crushed for three minutes in a carbon-steel mill to -300#. A 5g quantity of each sample was pressed into a 30mm diameter pellet with a boric acid packing under a pressure of 10 tons. The pellets were pre-pumped in a vacuum desiccator for 30 minutes prior to analysis to avoid cracking of the pellets in the spectrometer. A Philips PW1400 WDXRF spectrometer with a gold tube was used for the analysis of Pb, Cu and Zn. The instrument was run at 60KV, 45mA, using a LiF(220) analyser crystal and a fine collimator. Corrections were made for spectral overlap, tube contamination, background variations in mass and absorption coefficients.
Determination of the organic carbon content of the sediments was carried out by wet oxidation as outlined in the Walkley-Black method (Non-Affiliated Soil Analysis Work Committee, 1990).

Separation of a clay fraction from samples ZVC6A and ZVC7A was carried out by clay dispersion and subsequent flocculation to facilitate the analyses of the clay mineralogy by X-ray diffraction. The clay fraction was obtained by allowing the coarser fraction of the sediments to settle and then syphoning off the dispersed, suspended clay particles. Clay flocculation was induced by increasing the electrical conductivity of the suspension by addition of NaCl. The clay separate was dialysed for 48 hours to ensure complete removal of all the salt; after which the dense clay slurry was placed on a glass slide to allow the clay particles to settle out with a preferred orientation during slow drying by evaporation. The slide was glycerol-solvated by the spray method using a 15 % glycerol in water solution in order to facilitate identification of smectite peaks (Borchardt, 1989). This positive identification of smectite is facilitated by the expansion of the 1.45 nm inter-planar

spacing to 1.80 nm upon liquid glycerol solvation for montmorillonite, beidellite and nontronite (Borchardt, 1989).

The XRD analyses of the clay separates of samples ZVC6A and ZVC7A were carried out using a Philips DY 1870 X-ray diffractometer coupled with a Philips PW 1394 motor control, a Philips PW 1395 programmer and a Philips 1390 channel control. A Cu tube (CuKα $\lambda = 1.542$ A) was used operating at 40kV and 25mA. The samples were analyzed between 4°2θ and 30°2θ with a step size of 0.1°2θ and a step duration of 1 second.

3.2.2.2 Sorption experiments

Sediment samples ZVC6A and ZVC7A were chosen to represent the two end-member type sediments found in Zoar Vlei, i.e. a very fine-grained, organic-rich highly contaminated sample, and a sandier, organic-poor less contaminated sample, respectively.

3.2.2.2a *Sorption of Pb and Zn:*

Separate Pb and Zn solutions ranging in concentration from 10 to 500 mg/L were made up by dissolving $Pb(NO_3)_2$ and $Zn(NO_3)_2$ salts (PAL Chemicals; chemically pure reagent) in deionised water. Four sets of adsorption experiments were set up using sediment samples ZVC6A and ZVC7A. The sets were as follows:

Set 1: Pb solutions of the following concentrations (ppm) were added to ZVC6A: 10, 25, 40, 50, 60, 80, 100, 200, 300, 400 and 500.

Set 2: Pb solutions of the following concentrations (ppm) were added to sediment ZVC7: 10, 20, 25, 40, 50, 60, 80, 100, 200, 300, 400 and 500.

Set 3: Zn solutions of the following concentrations (in ppm) were added to sediment sample ZVC6A: 20, 30, 40, 60, 80, 100, 200, 300, 400 and 500.

Set 4: Zn solutions of the following concentrations were added to sediment sample ZVC7: 20, 30, 40, 50, 60, 80, 100, 200, 300, 400 and 500.

A 25 ml aliquot of either Pb or Zn solution was added to 2.5g of sun-dried, sieved sediment in a 50 ml centrifuge tube. The tube was corked and shaken on a reciprocal

shaker for 48 hours. Contamination or adsorption of Pb and Zn by the cork was prevented through the use of laboratory parafilm. The sediment slurry was then centrifuged using the IEC Centra - CL centrifuge at 6000 rpm for 10 minutes. The supernatant was analyzed for Pb and Zn by ICP-AES using a Jobin Yvon 70C spectrometer and J-Yess version 4.0 software. Fedgas 4.5 (95% Ar gas) was used at a flow rate of 12 l/min. The nebuliser flow rate was 2 l/min. The primary slit size and the secondary slit size used were 20 and 25 nm, respectively. The wavelengths used for the measurement of Pb and Zn were 220.353 and 213.856 nm, respectively. Three measurements were taken across the peak and 10 seconds was required for integration of the three readings. The pH of the supernatant was recorded using a Crison micro pH2001 pH meter.

3.2.2.2b *Desorption of Pb and Zn:*

25 ml aliquots of deionised (for Pb desorption) or vlei water (for Zn desorption) were added to the solid phase remaining after centrifugation in the adsorption experiment. Centrifuged supernatants were analysed for Pb and Zn as described above.

3.2.2.2c *Salinity dependence of Pb and Zn adsorption and desorption*:

25 ml aliquots of solutions containing 100 mg/L of either Pb or Zn and varying NaCl concentrations ranging from that representing fresh water to sea water (28g NaCl/L) were added to 2.5g sediment sample ZVC6A. The following concentrations (g NaCl/l) of NaCl solutions were used: 2, 4, 6, 8, 10, 12, 16, 20, 24, 28.

Equilibration and analysis of centrifuged supernatants for Pb or Zn was then performed as described above. The above procedure was repeated using NaCl containing no Pb or Zn in order to investigate the capacity of saline solutions to induce desorption of Pb and Zn.

3.2.2.2d *Investigation of the pH dependence of Pb and Zn desorption*:

Sample ZVC2A was used in this experiment due to limited availability of material, as it is similar to sample ZVC6A in terms of organic matter content, grain size distribution and level of transition metal contamination. Twelve 2.5g quantities of

sieved, sun-dried sample were each shaken for 48 hours with a 25 ml aliquot of vlei water, each aliquot having been acidified using 0.01M HCl to a different pH ranging between 3.5 and 7.5. The pre-equilibrium pH of the twelve acidified vlei water aliquots was as follows: 7.48, 7.08, 6.71, 6.48, 6.24, 6.00, 5.73, 5.5, 5.23, 5.02, 4.25, 3.6. Centrifuged supernatants were analysed for Pb, Zn and pH as described above.

3.2.2.2e *Investigation of acidity induced desorption of Pb and Zn using nitric acid:*
25 ml aliquots of nitric acid, ranging in concentration from 0.01M to 0.25M were shaken with 2.5g of sediment sample ZVC6A for 48 hours. The same procedure as above was then followed.

3.3 Results

3.3.1 Sediment analysis

The results of the Pb, Zn and Cu sediment analyses by XRF and the determination of sedimentary organic carbon by wet oxidation are presented in Appendix 1. These results include samples analyzed by Board (1993) and Farmer (1993). Concentrations of Pb, Zn and Cu vary from 4.1, 7.8 and 4.1 ppm respectively to unusually high concentrations of 472, 5183 and 108 ppm, respectively. Trace metal concentrations are thus highly variable, the highest metal contents existing in the uppermost sediment layers; a strong indication that the trace metal enrichment is anthropogenic.

The trace metal pollution components (Pb, Zn and Cu) were analyzed by various statistical procedures in order to assist in the explanation of their behaviour in the vlei. The Statgraphics package on the Earth Sciences HP9000 computer system was used to perform these analyses. Calculation of parametric statistical parameters was performed on the entire data set and on surface samples only and the results are presented in Appendices 7 and 8, respectively. It is evident that the data are not normally distributed, all trace metal variables showing no tendency to cluster and illustrate skewness towards higher concentrations. This non-normal behaviour of pollution components is an indication that the measured components are in reality not continuous and random, i.e. the variability is a real reflection of the variability

in either the distribution of the source of the pollution, or the variability in the characteristics of the sediment responsible for trace metal uptake. The positive skewness of the variables indicates that the sediments have been subjected to anthropogenic contamination by Pb, Zn and Cu.

Non-parametric Spearman Rank Correlation coefficients were calculated to investigate the association of the components (Appendix 9) and reveal that Zn, Cu, Pb and organic carbon are highly correlated at the 99% confidence level (p value = 0.0001). The mutual association of the trace metals indicates that the areal distribution of the sources of these metals are similar and that the metals are taken up and concentrated in the sediments by similar processes. Bivariate plots of Pb, Zn and Cu versus the percentage of organic carbon are presented in Figures 3.1a, b and c respectively. All three plots illustrate a significant positive correlation at the 95% confidence level, between trace metal and organic carbon content. Cu and Pb are highly correlated with organic carbon, Cu slightly more so than Pb; the correlation with regard to Zn is meaningful but significantly weaker than for Pb and Cu. The strong positive correlations provide no indication of a direct organic matter-metal binding mechanism, but merely suggest a mutual association of the two variables. The results are consistent with the sequential extraction data presented by Board (1993) and Farmer (1993). Lead is approximately evenly distributed between the oxide phases and the organic matter and sulphide phases, anthropogenic Cu is almost entirely associated with the organic matter/sulphide fraction, and Zn occurs in all speciation fractions but is predominantly bound to Fe and Mn oxides (Board, 1993).

The highest trace metal concentrations in the sediments of Zoar Vlei are encountered at the entrance of the southern pan on the Paarden-Eiland side of the vlei. This region of the vlei is exceptionally overgrown with grass and reed knolls creating stagnant pools, thereby enhancing and concentrating metal entrapment in the sediment. The sediments at the entrance of the southern pan are enriched in Pb, Cu and Zn relative to those in the emerging channel.

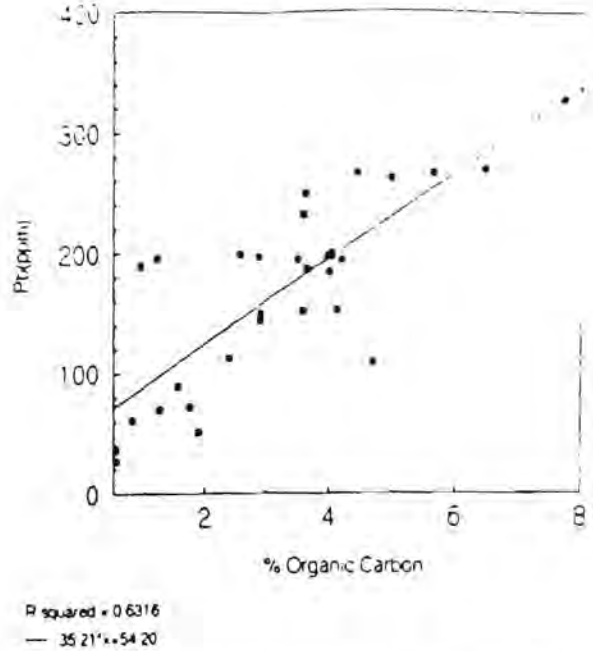

Figure 3.1a. Correlation between the Pb and organic carbon content of the sediments.

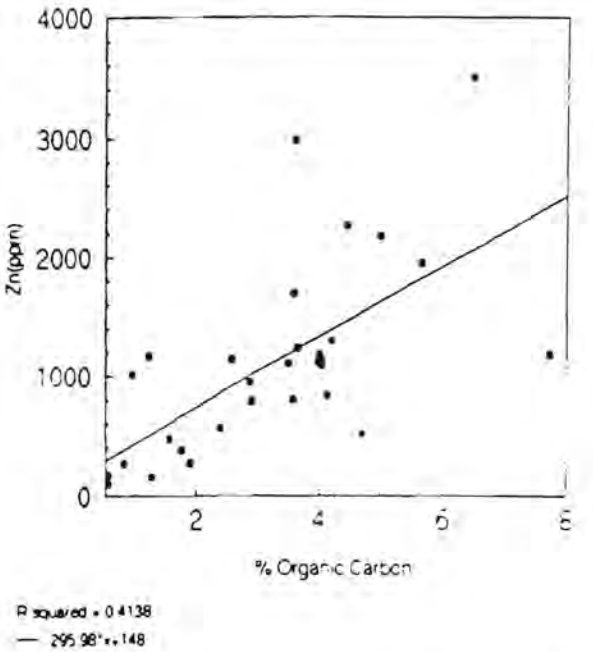

Figure 3.1b. Correlation between the Zn and organic carbon content of the sediments.

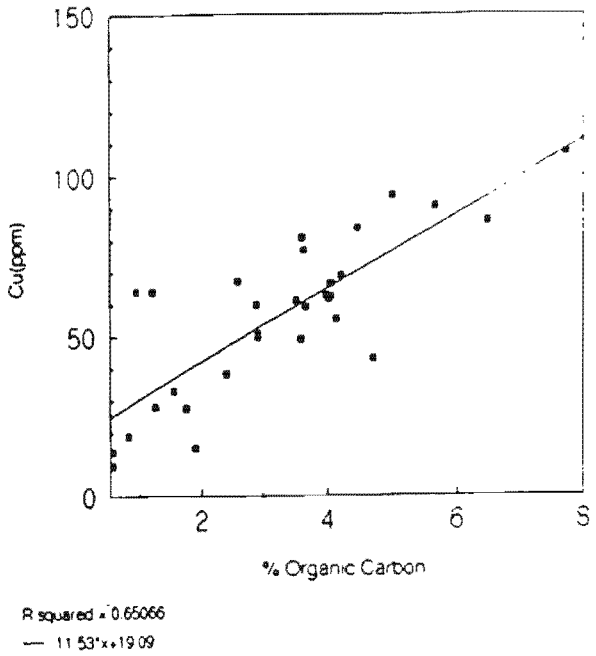

Figure 3.1c. Correlation between the Cu and the organic carbon content of the sediments.

Metal concentrations in the southern channel are highest at the point of emergence, and decrease rapidly downflow. The relatively low concentrations recorded in the sediments at and downflow of stormwater drains from the residential area, as well as the steady decrease in metal contamination in a northerly direction suggest that the pollution source is not residential. However caution must be employed when attempting to infer information regarding the source of the contamination from whole sediment elemental analyses, as the composition of the sediment controls its potential for contamination. The difference in the trace metal content of the sediment samples could either be the result of a lower adsorptive capacity of the sandier sediments, or it could indicate that the source of the pollution is at the southern end of the vlei system.

In the southern pan, metal concentrations appear to be slightly elevated on the industrial side of the vlei relative to the residential side. The proposed non-equivalence of the two samples was tested using the non-parametric Mann-Whitney U test, to determine whether the sediments from the industrial side are more contaminated than those on the residential side. The results of the statistical analyses

are presented in Appendix 10a and reveal that the two samples (ie residential and industrial) are not significantly different with respect to all three metals at a confidence level of 90%.

There is a strong trend of decreasing metal concentrations in a northerly direction in the vlei system. Results of a Mann-Whitney U test (see Appendix 10b) indicate that metal pollution in the northern pan is significantly lower than that in the southern pan at the 98% confidence level. The interconnecting channel belies this trend of decreasing metal contamination in the downflow direction and is relatively enriched in Pb, Zn and Cu. This is possibly a consequence of the highly vegetated, slow-flowing and muddy nature of the channel, the fact that there is a stormwater outlet from both the residential and industrial areas into the interconnecting channel, and possibly also that in the dry season water containing high concentrations of metals collects in stagnant, concentrated evaporation ponds in the channel, thereby providing excellent conditions for metal uptake by the sediments. The reasons for the lower levels of metal pollution in the northern pan are unclear. There are numerous stormwater drain inlets into the northern pan, so either the metal source lies in the south of the vlei system and metals are effectively removed from solution by the sediments prior to reaching the northern pan, or the sandier nature of the northern pan sediments (Board, 1993), and the fact that they contain less organic carbon has resulted in a smaller capacity for metal uptake. The latter suggestion implies that the northern pan sediments are saturated with respect to trace metals.

The XRD results for the analysis of the clay mineralogy in two glycerol solvated sediment samples, ZVC6A and ZVC7A, are presented in Appendix 2. The diffractograms for each sample are almost identical, thus the vastly different sedimentological properties are not due to variation in mineralogy, but to variability in the proportions of the sedimentary components. The dominant clay mineral in both samples is kaolinite ($Al_2Si_2O_5(OH)_4$), easily diagnosed by the presence of the very intense 0.716nm peak and the 0.357nm peak corresponding to the (001) basal plane first order reflection (peak 2) and the (002) basal plane second order reflection (peak 6) respectively (Dixon, 1989). The diagnostic kaolinite peaks described above

are more intense in the diffractogram obtained from the analysis of ZVC7A. Quartz is present in the clay size fractions of both samples in similar proportions, identified by the very intense (100) peak at 0.334nm (peak 7 on ZVC6A diffractogram, peak 6 on ZVC7 diffractogram) and the weak 0.426 nm peak (peak 4). The intensity ratio of the (100) peak (d=0.426 nm) to the (101) peak (d=0.334 nm) is 4.08 for sample ZVC6A and 5.26 for sample ZVC7. The high intensity ratio suggests that the (100) prism faces are well-developed, which, in a slide with a preferred orientation brought about by settling and evaporation, results in the majority of quartz grains lying with their *c* -axes parallel to the slide (Drees *et al.*, 1989). This suggests that the quartz grains present in the sediment have well-formed crystal faces and have not been subjected to sedimentological processes for long periods. Peak 1 in both difractograms is indicative of mica group minerals (Fanning *et al.*, 1989). The 0.51 nm peak (peak 3) confirms the presence of "mica" in both sediment samples and suggests that the "mica" is of the potassic, calcic and sodic variety rather than the biotitic variety (Fanning *et al.*, 1989). The term illite is applicable to such a "non-expanding, dioctahedral, aluminous, potassium mica-like mineral which occurs in the clay size fraction."(Fanning *et al.*, 1989). The very broad peak present in both diffractograms at approximately 1.8 nm is diagnostic of smectites after liquid glycerol solvation (Borchardt, 1989). The swelling properties of these 2:1 layer silicates are exploited for diagnostic purposes. Glycerol application causes the expansion of the 1.45 nm basal spacing, diagnostic of smectite at 54 % humidity, to 1.8 nm (Borchardt, 1989). The very broad peak is a result of incomplete expansion of all 1.45 nm basal spacings. Thus, smectite is present in both sediment samples in minor amounts and is likely to be partly responsible for the swelling properties of the sediments.

3.3.2 Sorption

It is important to note that the adsorption experiments were carried out using a "black box type" approach. Therefore only very tentative suggestions regarding the processes and mechanisms of adsorption can be made. As a consequence of complex formation in solution, metal adsorption is a competition between the free metal ions, the charged complexes containing the metal, and the complex-forming species themselves for sites on the surface. There can, therefor, be no quantitative prediction

possible regarding the extent of metal adsorption unless the equilibrium constants are known for every possible interaction (Mott, 1988).

3.3.2.1. Sorption of Pb and Zn by the sediments:

The results of experiment 3.2.2.2a are illustrated in Table 3.1 and in Figure 3.2 in the form of adsorption isotherms. An adsorption isotherm is a graph of the concentration of the species adsorbed (q_i) against the concentration of that species in solution once equilibrium has been attained (c_i). The slope of the adsorption isotherm at a given adsorptive concentration is a measure of the tendency of the species to be adsorbed. Thus the slope at a given concentration is the distribution coefficient, K_D, for the adsorption reaction. Adsorption reactions in soils and sediments are typically rapid, operating on time scales of minutes or hours in the case of readily exchangeable ions, and in the case of specifically adsorbed ions exhibiting long-term "tails" over days or weeks (Sposito, 1989). Thus it can be assumed for all practical purposes that equilibrium was attained after the 48 hour experimental duration period. Adsorption isotherms illustrate the influence of adsorptive concentration on the amount adsorbed. Of the two sediment samples used in this experiment, sediment ZVC6A contains significantly more organic carbon (7.72 % as opposed to 1.25 % in sample ZVC7A), and a greater proportion of silt and clay than sample ZVC7A. Table 3.1 reveals that both sediment samples have an extremely high affinity for Pb. This information, if plotted as an adsorption isotherm, would reveal an H-*curve* isotherm as described by Sposito (1989), who suggests that this condition is produced by either inner-sphere surface complexation or by van der Waals interaction in the adsorption process. The initial vertical slopes suggest that K_D for the adsorption of Pb for both sediment samples is exceptionally large and the accuracy by which it can be calculated is limited by the Pb detection limit for the analytical procedure used. From Table 3.1 it is evident that both sediment samples have a greater affinity for Pb than for Zn, as a greater proportion of Pb is adsorbed at approximate adsorbate concentrations. Sediment sample ZVC7A has a greater affinity for Zn than sample ZVC6A.

Table 3.1. Pb and Zn added to and adsorbed by sediment samples ZVC6A and ZVC7.

Sample	Pb added	Pb sorbed	% sorbed	Zn added	Zn sorbed	% sorbed
ZVC6A	0.483092	0.4809	99.55	15.29286	14.152	92.54
	2.898551	2.8929	99.81	61.17143	55.0237	89.95
	14.49275	14.4907	99.99	9.175715	8.5453	93.13
	3.864734	3.8647	100.00	76.46429	66.9215	87.52
	4.830918	4.8304	99.99	3.058572	1.6516	54.00
	9.661836	9.66	99.98	12.23429	8.457	69.13
	24.15459	24.1518	99.99	45.87857	39.3026	85.67
	2.415459	2.413	99.99	30.58572	23.0922	75.50
	19.32367	19.3211	99.99			
	1.207729	1.2056	99.82			
	1.932367	1.9311	99.93			
	2.8986	2.8986	100.00			
ZVC7A	0.483092	0.4822	99.82	7.646429	7.6232	99.70
	2.415459	2.4131	99.90	6.117143	6.0648	99.14
	14.49275	14.4788	99.90	12.23429	12.1584	99.38
	1.932367	1.9305	99.90	30.58572	30.1728	98.65
	0.966184	0.9653	99.91	3.058757	3.0032	98.19
	4.830918	4.8263	99.90	4.587857	4.4911	97.89
	9.662836	9.6525	99.90	15.29286	15.2305	99.59

	3.864734	3.861	99.90	76.46429	75.1517	98.28
	1.207729	1.2059	99.85	9.175715	9.1282	99.48
	19.32367	19.3023	99.89	61.17143	57.7458	94.40
	24.15459	24.1243	99.87			
	2.8959	2.8958	99.91			

All concentration units are mmol/kg

Figure 3.3 illustrates that Pb adsorption by the sediments induces Zn desorption for sample ZVC6A where the quantity of Zn released into solution by the sediment increased linearly with an increase in the amount of Pb adsorbed. However, the quantity of Zn released into solution is minor when compared to the Pb adsorbed which induced that Zn desorption. For example 24.15mmol/kg adsorbed Pb caused a release of 5.922 mmol/l Zn. The Zn adsorbed by sediment sample ZVC7A is less easily displaced by Pb adsorption.

Figure 3.2 illustrates Zn adsorption isotherms for the two sediment samples. The adsorption isotherm for sample ZVC6A is an L-curve isotherm which is characterised by a constant initial slope, i.e. the slope does not increase with the concentration of the adsorptive element in solution. This curve is the result of a high relative affinity of the sediment particles for the adsorbate. This affinity is lowered, however, with a decreasing amount of adsorbing surface remaining as the surface excess of the adsorbate increases (Sposito, 1989). The initial K_D for the Zn adsorption reaction by sediment sample ZVC6A, applicable up to an adsorptive concentration of approximately 40mmol/kg is 1.182 as illustrated in Figure 3.4.

The mathematical description of the L-curve isotherm either takes the form of the Langmuir equation or the van Bemmelen-Freundlich equation. The Langmuir equation has the following form:

$$q_i = bKc_i/1+Kc_i$$

where b represents the value of q_i that is approached asymptotically as c_i becomes

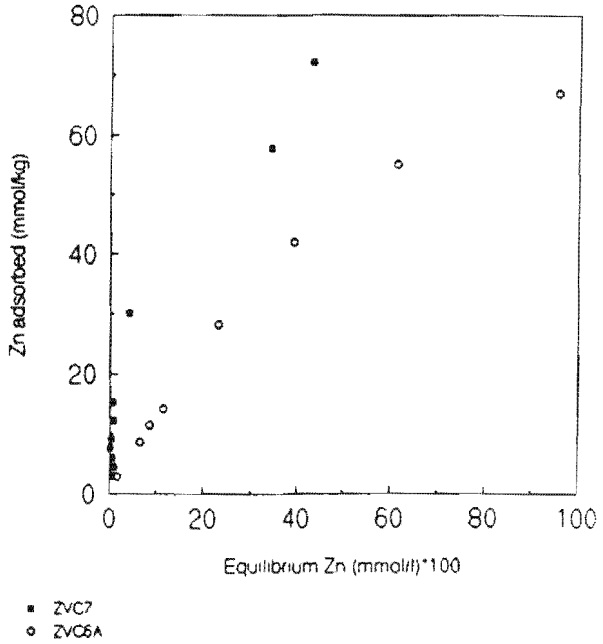

Figure 3.2. Zn adsorption isotherm for samples ZVC6A and ZVC7 obtained from the results of experiment 3.2.2.2a.

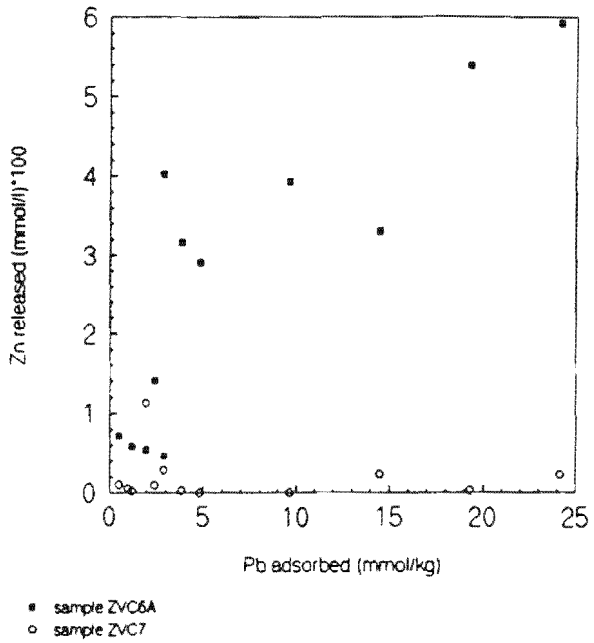

Figure 3.3. Pb adsorption causes Zn desorption. Plotted from the results of experiment 3.2.2.2a.

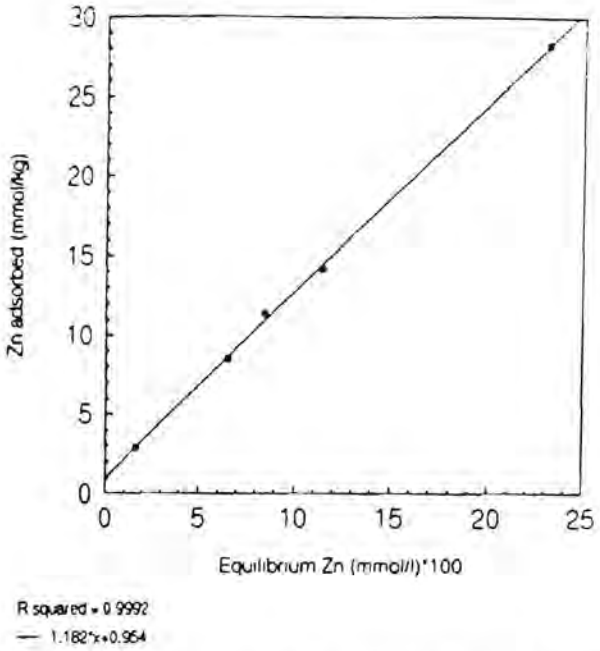

Figure 3.4. Determination of the initial slope of the Zn adsorption isotherm for ZVC6A.

arbitrarily large, and K determines the magnitude of the initial slope of the isotherm. The above equation may be expressed in the following form:

$$K_D = bK - Kq_i$$

in which case a graph of K_D against q_i is a straight line with a slope equal to -K and intercept equal to bK (Sposito, 1989).

The van Bemmelen-Freundlich isotherm equation has the following form:

$$q_i = Ac_i^B$$

where A and B are adjustable parameters and B is constrained to lie between 0 and 1. Thus a graph of log q_i against log c_i is a straight line with a slope B and an intercept log A (Sposito, 1989). To determine whether the L-curve isotherm in Figure 3.2c is a Langmuir or a van Bemmelen- Freundlich isotherm, graphs of K_D vs q_i and log q_i vs log c_i were constructed and are presented in Figure 3.5. A better fit was obtained for the van Bemmelen-Freundlich isotherm where, B = 6.338 and A = 80.721.

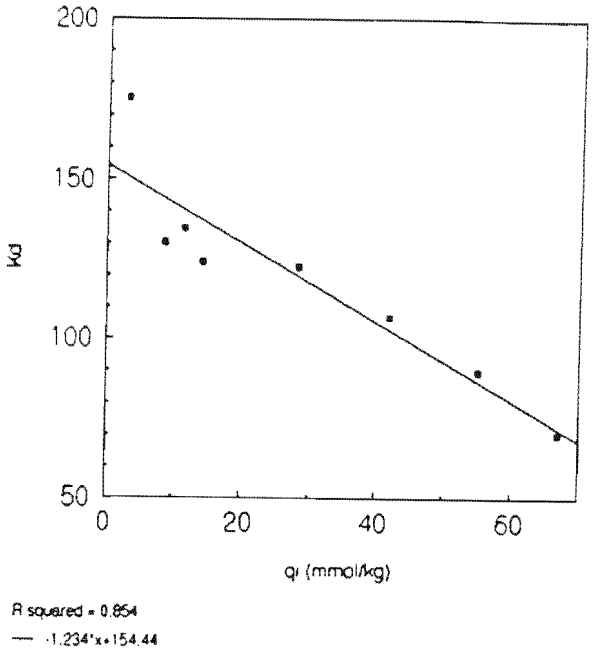

Figure 3.5a. Langmuir isotherm plot for Zn adsorption by ZVC6A.

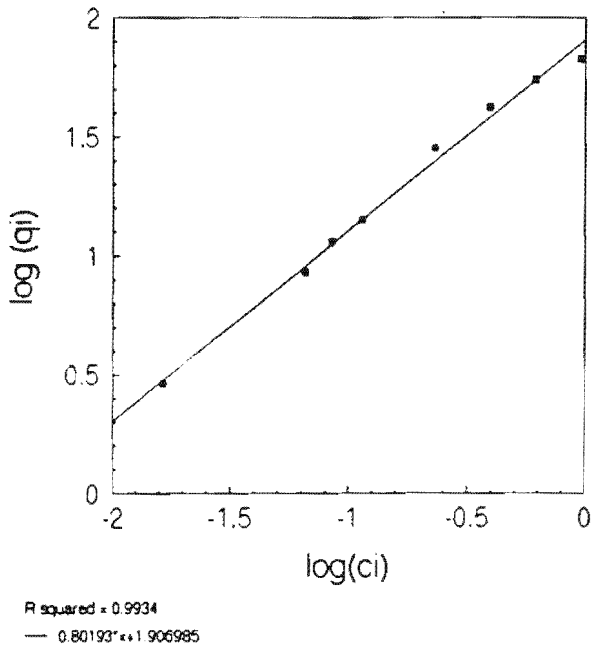

Figure 3.5b. Van Bemmelen-Freundlich isotherm plot for Zn adsorption by ZVC6A.

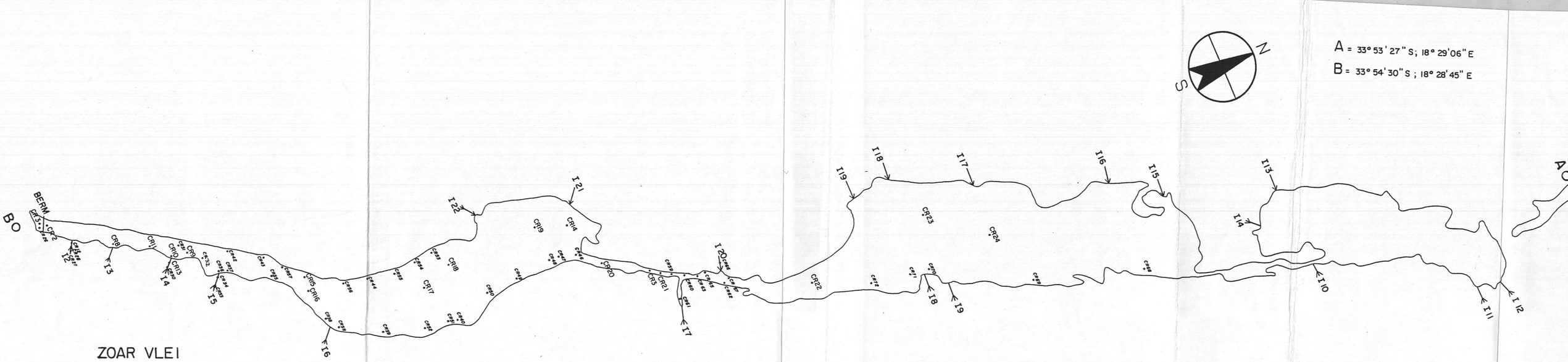

MAP 3. THE DISTRIBUTION OF WATER SAMPLING POINTS

Sediment sample ZVC7A illustrates a greater tendency to adsorb Zn than ZVC6A, as indicated by the steeper initial slope of the adsorption isotherm. The isotherm is an intermediate between an H-curve and an L-curve. The initial slope of the curve is vertical, indicating a very high initial K_D applicable for a maximum adsorptive concentration of approximately 15mmol/kg. At adsorptive concentrations greater than 15mmol/kg, K_D declines rapidly.

3.3.2.2. Desorption of Pb and Zn:

The results of the desorption experiments described in section 3.2.3.2 are presented in Figure 3.6. Consistent with the results displayed in Figure 3.3, the Zn adsorbed by ZVC7A is less easily desorbed, i.e. the forces binding the adsorbent to the sediment particles of ZVC7A are greater than those for ZVC6A. However, both sediment samples illustrate that Zn adsorption is largely irreversible and that the degree of reversible adsorption increases in a manner convex to the x axis with increasing metal adsorbed. Pb adsorption was observed to be completely irreversible.

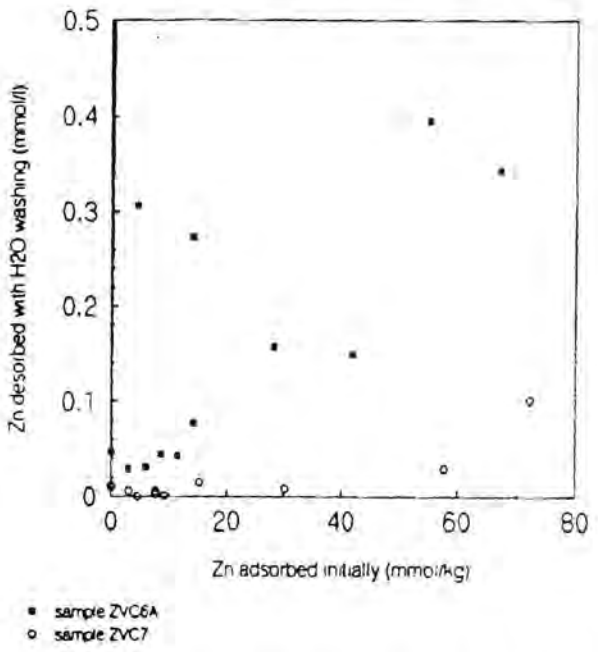

Figure 3.6. Amount of Zn desorbed with H_2O washings vs Zn adsorbed. Plotted from the results of experiment 3.2.2.2b.

3.3.2.3. The effect of salinity on Pb and Zn sorption and desorption:

The salinity dependence of Zn and Pb adsorption by sample ZVC6A was investigated as described in 3.2.2.2c and the results are presented in Figure 3.7. The effect of salinity on Pb adsorption is negligible, as all the dissolved Pb remains bound by the sediment regardless of the salinity of the solution. However, salinity has a weak influence on Zn adsorption as is illustrated in Figure 3.7. Maximum Zn adsorption is achieved at a salinity of 8g NaCl/l. The amount of Zn adsorbed increases with increasing salinity for dilute solutions (up to 8g NaCl/l), and decreases with increasing salinity exceeding 8g NaCl/l. There is an equal tendency for Zn to be

removed by adsorption from solutions approximating fresh water and sea water (28g NaCl/l, 0.5M NaCl). However the influence of salinity on adsorption processes appears small. Variation in liquid phase salinity over the entire natural range results in a variation of Zn adsorption of 8.99 ppm corresponding to 8.99 % of the total Zn available for adsorption. No desorption of either Pb or Zn could be induced by equilibration of the sediment with saline solutions. This indicates that the influx of saline water from the Milnerton Lagoon into Zoar Vlei would not cause metal release from the sediments.

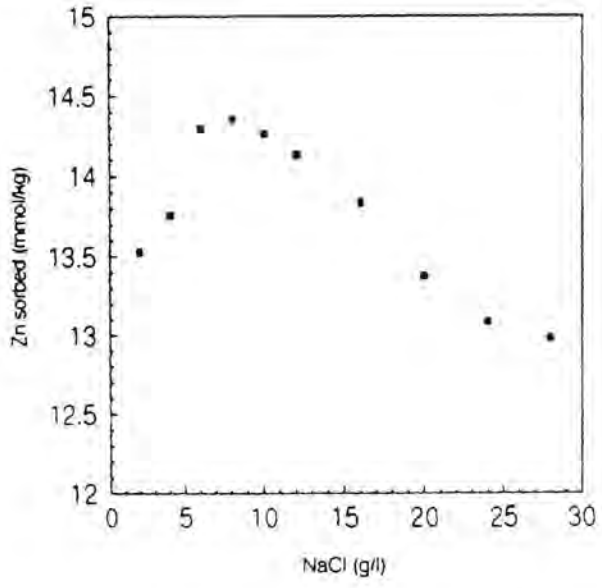

Figure 3.7. The effect of salinity on Zn adsorption by sample ZVC6A. Plotted from the results of experiment 3.2.2.c.

3.3.2.4. Acidity induced desorption of Pb and Zn:

The results of experiments 3.2.2.2d and 3.2.2.2e, i.e. the investigation of acidity induced desorption using vlei water acidified with HCl and nitric acid, respectively, are presented in Figure 3.8. In both cases a significant negative correlation between pH and Zn desorption is observed. The pH recorded in experiment 3.2.2.2d and plotted in Figure 3.8a is the pH of the vlei water after acidification with HCl prior to addition to and equilibration with the sediment. This experiment was designed specifically to model the consequences of an acid spill into Zoar Vlei. Equilibration of the liquid phase with the sediment neutralised the liquid phase acidity, indicating the large acid neutralising capacity of the sediment. The final pH of the supernatant ranged between 7.8 and 7.2. Despite the neutralisation of the acidity, significant Zn desorption was induced. At an initial solution pH of 3.6, 23.5 ppm Zn, corresponding to 237.2 mg Zn per kg of sample was released into solution compared to 84.4 mg Zn per kg of sample (8.44 ppm) desorbed at an initially neutral pH. The pH dependence of Zn desorption illustrated in Figure 3.8a, may be expressed by the following equation: $y = -3.45x + 37.23$ ($R = -0.873$), where y = the Zn released into solution and x = the pre-equilibrium pH.

The pH dependence of desorption is more significant in experiment 3.2.2.2e, as illustrated in Figure 3.8b. This is due to the more concentrated nitric acid solutions used in this experiment. The pH recorded in Figure 3.8b, is the equilibrium pH of the sediment/liquid system. In contrast to the results for Zn, no Pb desorption could be induced by acidification in either experiment 3.2.2.2d or 3.2.2.2e.

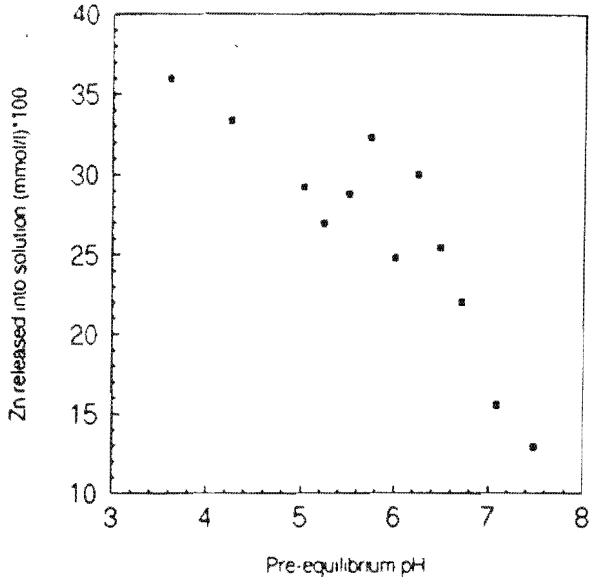

Figure 3.8a. Zn desorption from ZVC2A using vlei water acidified with HCl. Plotted from the results of experiment 3.2.2.2d.

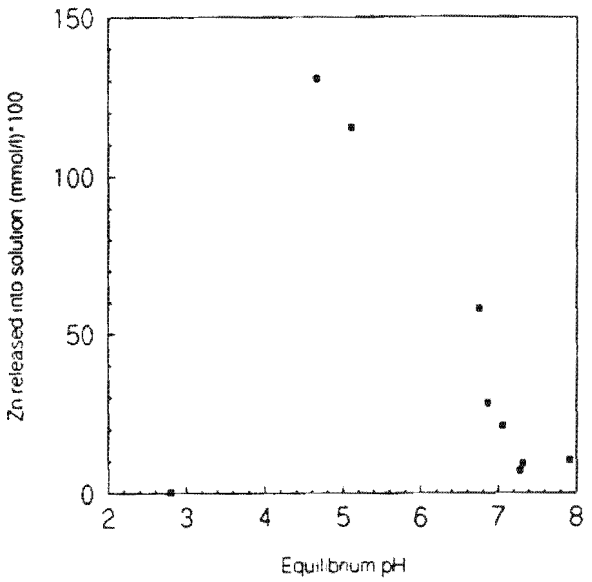

Figure 3.8b. Zn desorption from ZVC6A using nitric acid. Plotted using the results of experiment 3.2.2.2e.

3.4 Discussion

The X-ray diffraction results presented in section 3.3.1.3 indicate that the dominant clay mineral present in Zoar Vlei is kaolinite, which commonly represents the most stable end-weathering-product in mature soils and sediments. Weathering reactions deplete K^+ concentrations and increase acidity through leaching. Thus the direction of weathering is towards kaolinite formation from K-feldspar and K-mica (Dixon, 1989). Accessory quartz, illite and smectite are present in the clay fraction of the sediments. Illite originates predominantly from micaceous parent materials and tends to predominate in younger, less weathered environments. Smectites are usually present in soils or sediments in poorly drained regions, where smectite in the clay mineralogy is inherited from basic parent materials. The cation exchange capacities of kaolinite, illite and smectite are shown in Table 3.2. The fact that kaolinite has a low CEC and dominates the clay mineralogical composition indicates that the organic matter component of the sediment may be partly responsible for Pb and Zn sorption. However, due to the high CEC of smectites, their influence on sediment properties is proportionately very large.

Table 3.2. CEC for kaolinite, illite and smectite (values from Dixon, 1989; Fanning *et al.*, 1989; and Borchardt, 1989).

	CEC $cmol_c/kg$
kaolinite	< 20
illite	20 - 40
smectite	110

Based on the available evidence, it is not possible to attribute the observed uptake of Pb and Zn by the sediments to a particular process, or to determine which component of the sediment is responsible for the metal uptake. Uncertainty as to whether adsorption or precipitation is the dominant mechanism of removal of Pb and Zn is inevitable, as only the change in concentration of the relevant cations (Pb and

Zn) was measured. However, the adsorption isotherms presented in section 3.3.2 comply with the theoretical adsorption isotherm categories described by Sposito (1989). The smooth and predictable behaviour of the H-curve and L-curve isotherms suggests that a single process of removal of the cations from solution is active over the observed concentration ranges. Irregular adsorption isotherms would be indicative of several processes of Pb and Zn removal over limited concentration ranges (Mott, 1988). The components of the sediment capable of adsorbing Pb and Zn are clay minerals, Fe/Mn oxides which were identified in the field, sulphides and organic matter. The results of the adsorption experiments are consistent with what is known about adsorption by all the above categories, as all have a greater tendency to adsorb Pb than Zn (Forstner and Wittman, 1979).

Metal cations may be adsorbed onto a siloxane surface via three mechanisms: 1. the formation of inner sphere surface complexes; 2. outer sphere surface complexes which includes the cation solvation shell; and 3. via the formation of a diffuse ion swarm. The formation of an inner sphere surface complex involves incorporation of a cation into the siloxane cavity in 2:1 layer silicates and involves covalent and ionic bonding. This type of adsorption is termed specific adsorption; the formation of the adsorption bond is dependent on the electronic configuration of the adsorbate ions and the adsorbent surface functional groups. In the case of the formation of the diffuse ion swarm, the solvated ion does not form a complex with the charged surface functional group, but neutralises surface charge in a delocalised sense. The formation of a diffuse ion swarm and an outer sphere surface complex involves electrostatic bonding only, which is termed non-specific adsorption. Ions adsorbed by these mechanisms are readily replaced by leaching with an electrolyte solution of prescribed composition, concentration and pH and are,therefore readily exchangeable ions (Sposito, 1989).

All the adsorption isotherms presented in section 3.3.2 indicate that the sediment has a greater adsorptive capacity and affinity for Pb than for Zn. This observation supports theoretical considerations regarding the relative tendency of free metal cations to form inner sphere surface complexes with a siloxane surface. Pb^{2+} has a

greater ionic radius than Zn^{2+} and thus creates a smaller electric field, with the result that Pb^{2+} is less likely to remain solvated than Zn^{2+} and istherefore available for the formation of inner sphere surface complexes. The electronic configuration of Pb^{2+}, being a larger ion than Zn^{2+}, is more easily distorted, thus compatibility between the cation electronic configuration and that of the surface functional group is more easily achieved (Sposito, 1989). In contrast with the above reasoning, preferential adsorption of heavy metal hydroxy species is suggested by the fact that the pH edge of adsorption of various heavy metals by clay minerals closely mirrors the onset of the formation of the respective heavy metal hydroxy species in solution (Jean and Bancroft, 1986). The above phenomenon will be addressed in chapter 4 where speciation data will be presented for Pb and Zn using the MINTEQA2 computer speciation programme in order to determine whether the preferential adsorption of Pb at neutral pH could possibly be explained by a greater tendency for the formation of lead hydroxy species than zinc hydroxy species.

Farrah *et al.* (1980) investigated adsorption of Pb and Zn by Na-saturated kaolinite, illite and montmorillonite at a pH of 5 and showed (in contrast to the results of this study) that the effect of concentration on adsorption can be described by a Langmuir isotherm. The discrepancy between the results of this study and those of Farrah *et al.* (1980) are perhaps due to the fact that the adsorbate concentrations used in this study were very much lower. Therefor, the isotherms that appear to be H-*curve* isotherms could in fact be L-*curves* when extended to higher adsorbate concentrations and the availability of adsorption sites becomes limiting. The affinity for metal cations of the Zoar Vlei sediments, particularly for Zn is lower than that of the pure clays investigated by Farrah *et al.* (1980). Although a particle size analysis of the sediment was not undertaken, a tentative suggestion may be made that the lower affinity of the Zoar Vlei sediments for Pb and Zn may be due to dilution of the sediments with silt and sand which has a relatively lower adsorption capacity.

Adsorption of trace metals by Fe/Mn oxides is influenced by surface charge which is a function of the pH and ionic strength of the equilibrium solution (Schwertmann and Taylor, 1989; Mc Kenzie, 1989). In the presence of water, the Fe and Mn ions

located at the surface of an oxide become completely hydroxylated through bonding an OH^- group to each surface metal ion. Polar water molecules are then adsorbed onto this hydroxylated layer through H-bonding forming a surface monomolecular water layer (Dixon and Weed, 1988). Positive or negative surface charge is created by adsorption or desorption of H^+ or OH^- ions by the hydrated surface layer. Thus the surface charge of Fe and Mn oxides is pH dependent. This excess surface charge is balanced by adsorption of cations or anions onto the outer part of the electric double layer, ions which are readily exchangeable. The point of zero charge (PZC) for all Fe oxides ranges between 7 and 9 pH units, while that of Mn oxides ranges from 1.5 to 4.6 pH units (Dixon and Weed, 1989). Therefore at the approximately neutral pH at which the adsorption experiments were conducted, the surface charge on the Fe oxides may be considered small if not negligible, and the Mn oxide surfaces were significantly negatively charged. Both Mn and Fe oxides have a strong tendency to specifically adsorb Pb and Zn and both show a greater affinity for Pb than for Zn in agreement with the adsorption results presented in this study. This tendency is more strongly expressed by Mn oxides as a result of the low PZC and resultant large negative surface charge. This was illustrated by Balistrieri and Murray (1986), where it was shown that Pb and Zn adsorption was positively correlated with the Mn content of the sediment. The pH dependence of adsorption of heavy metals by Fe and Mn oxides is a combination of the effect of pH on oxide surface charge, and the pH dependence of the formation of heavy metal hydroxy ions in solution which are believed to be adsorbed preferentially to free divalent ions (Dixon and Weed, 1988).

Board (1993) and Farmer (1993) showed through the use of a sequential extraction procedure (Tessier *et al.* 1979) that sediment organic matter and sulphide phases are particularly important with regards to Pb complexation. The sediments used in the adsorption experiments were oxidised, therefore the possibility of metal complexation to sulphides is eliminated. However, organic matter plays a major role in metal cation and proton exchange reactions as discussed in chapter 1.

The adsorption results of experiments 3.2.2.2a and 3.2.2.2b presented in section 3.3.2

indicate the following:

The sediments in Zoar Vlei have a greater affinity for Pb than for Zn. This is particularly evident regarding sample ZVC6A, despite the fact that the concentration of Zn used in the adsorption experiments exceeds that of Pb. The maximum adsorption of Pb achieved in experiment 3.2.3.1 is 25 mmolPb/kg which appears to be well below the adsorption capacity of the sediments for Pb. The initial Pb content of samples ZVC6A and ZVC7A was 1.573 mmolPb/kg and 0.338 mmolPb/kg respectively. Thus the Pb presently adsorbed by the sediments in the vlei is negligible in comparison to their capacity for Pb. Pb adsorption by the sediments is specific and selective in nature, as illustrated by the irreversibility of the adsorption process and by the selective exchange of Pb for Zn in adsorption sites as shown in Figure 3.3. This suggests that Pb adsorption involves the formation of covalent bonds between the metal cation and the siloxane cavity in the case of adsorption by 2:1 layer silicates, the penetration of the Fe or Mn co-ordination shell and the formation of a covalent bond with the structural atom via O and OH groups in the case of adsorption by Mn and Fe oxides, and formation of a covalent bond between the adsorbate and surface function groups of the adsorbent. Experimentally determined K_D values for Pb and Zn adsorption by samples ZVC6A znd ZVC7A are reported in Table 3.3. The very high experimentally determined distribution coefficients K_D for Pb adsorption suggest that all the Pb introduced into the vlei in solution will be adsorbed by the sediments. The irreversibility of this adsorption even under acidified conditions (experiments 3.2.2.2d and 3.2.2.2e) indicates that the sediments provide a permanent storage facility for Pb. The tendency for Pb to be adsorbed by both sediment samples is equivalent at the investigated adsorbate concentrations. Sample ZVC7 contains significantly more sand and less clay and organic carbon than sample ZVC6A (1.25 % organic carbon compared to 7.25 % in sample ZVC6A). The equivalent affinity of the two samples for Pb, and the fact that the adsorption capacity of both samples for Pb was not approached in the experiments, suggests that the lower initial Pb content of the sandier sediment which was sampled from the northern pan (ZVC7, see map 1) is resultant from dilution of the dissolved Pb further away from the source and removal of the majority of the Pb from solution by sediments closer to source.

Table 3.3. Calculated distribution coefficients K_D for Pb and Zn adsorption by sediment samples ZVC7 and ZVC6A. The specific K_D values for the different adsorption concentration ranges are presented in the Appendix 3.

Metal adsorbed	Sediment sample	Conc. range (mmol/kg)	K_D
Pb	ZVC7A	0-14 14-19 19-25	not measurable 70165 34712
Pb	ZVC6A	0-25	large, ranging from 21.66 to 909.9
Zn	ZVC7A	0 - 15	>500
Zn	ZVC6A	0 - 30	1.182

The Zn adsorption isotherms presented in Figure 3.2 illustrate the following: Sediment sample ZVC7A illustrates a greater affinity for Zn than does sample ZVC6A. Thus the sandier sediment containing less organic matter appears to adsorb Zn more efficiently than sample ZVC6A. This arises from the fact that sample ZVC6A has an initial Zn concentration of 18.11 mmol/kg compared to 2.40 mmol/kg Zn in sample ZVC7A. The maximum concentration of Zn adsorbed by ZVC6A is 66.85 mmol/kg compared to 72.15 mmol/kg by sample ZVC7A. Thus the total concentration of Zn, after maximum adsorption that was achieved in this experiment had occurred for samples ZVC6A and ZVC7A, is 84.96 mmol/kg and 74.55 respectively. The decrease of the slope of the adsorption isotherm at high adsorbate concentrations is more marked for sample ZVC6A than ZVC7A. This is shown in Appendix 3, as the experimentally determined K_D value for Zn adsorption by sample ZVC6A is smaller than for that of ZVC7A. This indicates that the total capacity of sample ZVC6A to adsorb Zn is not significantly greater than that of sample ZVC7A, and this limiting capacity is approached in the adsorption experiment.

Figure 3.6 shows that a greater proportion of the Zn adsorbed by sample ZVC6A than that adsorbed by ZVC7A is desorbed simply by agitation of the sediment with distilled water. However, the degree of reversibility of adsorption remains low for both sediments. The irreversibility of adsorption indicates that Zn adsorption is specific in nature, and thus involves the formation of covalent and ionic bonds between the adsorbate and the surface functional group. The higher degree of reversible adsorption by ZVC6A suggests that specific Zn adsorption sites are limited and in this case exceeded, in which case the excess adsorbate is bound to the sediment particle surface purely by the Van de Waals forces between the negative surface charge and the cation in solution.

Due to the discrepancy between the concentrations of Pb and Zn used in the adsorption experiments, and the differing concentrations of Pb and Zn already existing in the sediments, one cannot arrive at conclusions regarding the relative capacity of the sediments for either metal. What has been made clear, however, is that the total Zn "carrying capacity" of the sediments in the vlei is already approached, whereas that for Pb is not. It is also impossible to determine the exact nature of the adsorption sites. However, the fact that Pb adsorption induces Zn desorption indicates that the same sites are capable of adsorbing both metals, and that Pb is preferentially selected and held more strongly than Zn by the adsorption site.

Figure 3.8 shows that acidification causes Zn but not Pb desorption from the sediment. This implies the following:

1. That a decrease in pH causes dissolution of the adsorbent responsible for Zn adsorption only. This suggestion is unlikely in the light of the evidence discussed in the previous section, as it implies that completely different substrates with different solubilities are responsible for Pb and Zn adsorption. The fact that Pb adsorption induces Zn desorption clearly indicates that this implication is unrealistic.
2. An excess of H^+ ions in solution influences the speciation of Pb in such a manner that the charged lead complexes are particularly partial to adsorption. The

dependence of adsorption on the speciation of the adsorbate which is a function of pH is well documented (Jean and Bancroft, 1986). This implies that Pb was initially released into solution, that the Pb^{2+} ions reacted with ions in solution under the acidified conditions and that the new Pb species were readsorbed.

3. The surface charge of clay minerals, oxides and organic matter varies with the concentration of H^+ and OH^- ions in solution. At low pH's the surface functional groups will be swamped with H^+ ions and the negative surface charge will be effectively neutralised (Dixon, 1989). Thus non-specific adsorption of cations will not be possible as it relies on the electrostatic attraction between a negatively charged surface and a positively charged ion or complex in solution. However specific adsorption may still occur if the initial electrostatic repulsion between the cation and the substrate is easily overcome. The fact that Pb remained adsorbed, when Zn was forced into solution implies that the nature of the attraction between the adsorption site and the Pb species does not rely on Van de Waals forces. It is covalent and significantly stronger than the H^+ - adsorption site bond that would replace it were Pb desorption to occur. One can therefore conclude that the Pb- substrate bond is stronger than the Zn-substrate bond.

The results of experiment 3.2.3.5 (shown in Figure 3.8) indicate that acidification of the vlei water causes significant Zn desorption. A pre-equilibrium pH of 3.6 of the aqueous phase caused the release of 6.7 % of the adsorbed Zn. However acidification of the vlei water by an acid spill would not induce significant Zn release due to rapid dilution of the acidity in the vlei. If Zn release were to occur, dilution of the dissolved Zn in the vlei water would eliminate the potential threat to the ecosystem. Long-term acidification of the vlei water by acid rain poses a more severe threat with respect to Zn release.

The results of experiment 3.2.2.2d show that the sediments have a considerable capacity to neutralise acidity. Thus the observed Zn desorption probably results from displacement of Zn by H^+ ions. For the most highly acidified sample a pH change of 3.63 was achieved (pH_i=3.6; pH_f=7.23) which corresponds to an uptake of 2.3442

mmol of H^+ per kg of sediment. 3.596 mmol/kg of Zn was released into solution in this experiment indicating that Zn release and associated neutralisation is not merely a simple ion exchange reaction.

The decrease in Zn adsorption with increasing salinity above 8g NaCl/l is explained by the preferential binding of Na^+ ions onto Zn adsorption sites at high Na^+ concentrations by mass action (Frenet, 1980). At the highest NaCl concentration used in this experiment the initial concentration of Na^+ ions in solution is 0.4796mol/l compared to a Zn concentration of 1.529 mmol/l. The large quantity of Na^+ ions present in salt water tend to saturate the surface sites, and the exchange selectivity is therefore weaker with regard to Zn ions than that shown with regard to Na^+ ions (Frenet, 1980). The fact that Pb adsorption is unaffected by the change in salinity of the liquid phase indicates that the exchange selectivity of Pb is stronger than that of Na^+ ions even at high Na^+ concentrations; the Pb ions occupy specific adsorption sites which are unavailable for Na^+ complexation. The initial increase of Zn adsorption with increasing salinity suggests that at low Na^+ ion concentrations exchange of Zn for Na^+ on adsorption sites is not the dominant process. Perhaps the formation of $ZnCl^+$ is favoured at lower Cl^- ion concentrations and is preferentially adsorbed. Maximum adsorption is achieved at a Cl^- ion concentration of 0.0685 mol/l.

The results of the experiment to investigate the effect of salinity-induced desorption indicate that no Pb or Zn desorption is induced by equilibration of the sediment with a saline solution (see appendix 7). Therefore sea water incursion into the vlei does not at the present time cause metal release and pose a threat to the ecosystem. Negligible concentrations of Zn were released into solution compared with the Zn release obtained in experiment 3.2.2.2b (Appendix 4c), suggesting that the Zn accumulated in sediment sample ZVC6A represents that which is stable under the conditions existing in the vlei, whereas the Zn adsorption occurring in the laboratory is less stable. However, one can conclude from the results of these experiments that the Zn contained in the sediments at the present time will not be affected by a change in the salinity of the vlei water, and that the capacity of the sediments to

adsorb Zn and Pb introduced into the vlei system is not affected by changes in salinity.

3.5 Conclusions

The following conclusions may be drawn on the basis of the findings of this report:

1. Pb and Zn have become significantly enriched in the sediments in Zoar Vlei through anthropogenic activities in the surrounding area. The extent of the trace metal pollution is greatest at the entrance of the southern pan on the Paarden-Eiland side of the vlei. The sediments adjacent to the semi-industrial area are not significantly enriched in trace metals relative to the rest of the vlei. The concentrations of Pb and Zn decrease significantly moving in a northerly direction through the vlei system. The above spatial distribution of Pb and Zn in the sediments is thought to be a reflection of an industrial source of the metals in the south of the vlei system.
2. The clay mineralogy of the sediments consists predominantly of kaolinite, with accessory amounts of quartz, illite and smectite.
3. The sediments in Zoar Vlei have a significant capacity to adsorb both Pb and Zn. The affinity of the sediments for Pb exceeds that of Zn, and Pb adsorption induces Zn desorption.
4. The Pb adsorption capacity of the sediments far exceeds the present concentration of Pb in the sediments, whereas the tendency of the sediments to adsorb Zn is limited by the availability of suitable adsorption sites at the present time. The fact that Pb uptake causes Zn release indicates that further influx of Zn or Pb into the vlei system poses a threat to the ecosystem with regards to Zn toxicity. The bioavailability and the effect of elevated concentrations of dissolved Zn on the aquatic life forms in the vlei requires investigation.
5. The high degree of irreversibility of adsorption of both Pb and Zn indicates that under the present environmental conditions the sediments act as a suitable storage facility for both Pb and Zn. Influx of saline water from the adjacent Milnerton Lagoon would not significantly influence the affinity of the sediments to adsorb either Pb or Zn, or induce trace metal release from the sediments.
6. Acidification of the vlei water causes Zn release from the sediments through

neutralisation reactions. Long term acidification of the vlei water could, therefore result in further Zn release. Based on the locality and characteristics of the vlei, acidification could ocurr through acid ingress into the vlei system via point or diffuse sources, or by drying and oxidation of the sulphide-rich sediments in the vlei and the associated production of sulphuric acid.

CHAPTER 4

Chemical composition and speciation of the vlei water

4.1 Introduction

Total water analyses including dissolved Pb and Zn concentrations are presented in this chapter. The need to determine dissolved concentrations of Pb and Zn in the vlei water was highlighted by Board (1993) and Farmer (1993) in order to assess the effectiveness of the sediments as a trace metal filtering system in preventing elevated concentrations of dissolved Pb and Zn from passing through the vlei and entering Milnerton Lagoon. Thus the main objectives of this chapter are the following:

1. To assess the quality of the vlei water, particularly with regard to concentrations of dissolved trace metals.
2. To determine whether Pb and Zn are entering the vlei in the dissolved form at the present time and to identify the source of the pollution.
3. To determine the speciation or association of ions in the vlei water, facilitating a better theoretical understanding of the adsorption mechanisms occurring at the sediment-water interface in the real situation and identifying the differences between real and experimental conditions.

4.2 Materials and methods

4.2.1 Sampling

Seventy-two vlei water samples were collected from the vlei and adjacent storm water drains, from early autumn prior to the winter rains, when the water lay in evaporation ponds, through to mid-winter when the vlei was full, in pre-rinsed plastic bottles. Sampling points were chosen so as to cover the entire area. Two samples were taken at each sample point. One of the samples from each site was acidified with concentrated nitric acid (55 %) to a pH of between 2 and 3 for subsequent cation analysis. This acidification was achieved by addition of the vlei water sample to nitric acid already in the sample bottle. The pH and electrical conductivity of the non-acidified samples were measured in the laboratory with the Crison micro pH2001 pH meter and the Crison Micro electrical conductivity meter, respectively, as soon

after sampling as possible. The samples were filtered through 0.45um Schleicher and Schuell membrane filter paper, and stored under refrigeration prior to analysis.

4.2.2 Water analysis

4.2.2.1. Dissolved organic carbon:

Dissolved organic carbon was determined on a filtered non-acidified sample, adjusted to pH approximately 3.5 using 0.1M perchloric acid, on a Anatoc Dissolved Organic Carbon Analyzer. This determination is based on the photocatalytic oxidation of dissolved organic carbon to carbon dioxide. The carbon dioxide is then bubbled through deionised water and the increase in the electrical conductivity of the water associated with the dissolution of the CO_2 is measured. Thus the amount of organic carbon oxidised can be determined.

4.2.2.2. Total alkalinity:

Total alkalinity (end-point pH=4.3) of the filtered non-acidified samples was determined by titration of a 25ml aliquot of sample against 0.01M HCl; screened methyl orange was used as an indicator and the end point was recognised by the colour change from pink to purple.

4.2.2.3. Anions:

The filtered non-acidified samples were analysed for total anions (Cl^-, SO_4^{2-}, NO_3^-, PO_4^{3-}, Br^- and F^-) using high performance ion liquid chromatography. Vlei water samples were diluted to EC < 100μS/cm with deionised water (MQ, filtered through millipores following deionisation). The Dionex DX300 series suppressed IC system was used coupled with the AI-450 chromatography software. The HPIC-AG4A and HPIC-AS4A-SC columns were used as the guard and separator columns, respectively. The eluent flow rate was 2.0 ml/min and suppressed by an anion MicroMembrane suppressor (AMMS). The eluent was a sodium carbonate and sodium bicarbonate mix (1.80mM Na_2CO_3; 1.70mM $NaHCO_3$).

4.2.2.4. Cations:

Analyses of 10 elements (Na, Ca, Mg, K, Pb, Cu, Zn, Cd, Fe and Al) were carried

out by ICP-AES. The spectrometer used is the Jobin/Yvon 70C; J-Yess version 4.0 software was used. Fedgas (4.5), 95% Ar gas was used at a flow rate of 12 l/min. The nebuliser flow rate for the analyses was 2 l/min. The primary and secondary slit sizes used were 20 and 25 nm respectively. The wavelengths used for the cation determinations are given in Appendix 11.

4.2.2.5. Investigation of the solubility of $PbCO_3$

$PbCO_3$ is the most sparingly soluble Pb compound; the solubility of Pb will be controlled either by equilibrium with $PbCO_3$ or by adsorption and co-precipitation phenomena. A white $PbCO_3$ precipitate was observed to form on addition of $Pb(NO_3)_2$(s) (PAL Chemicals, chemically pure reagent) to vlei water with an alkalinity of approximately 3mmol/l. The solubility of $PbCO_3$ was investigated by addition of varying amounts of $Pb(NO_3)_2$ salt to vlei water containing a total alkalinity of approximately 3mmol/l. The resulting $PbCO_3$ suspension was centrifuged using the IEC-Centra - Cl centrifuge at 6000 rpm for 20 minutes and the supernatant was analyzed for Pb by ICP-AES using the same instrumental parameters as described in experiment 3.2.2.2a.

4.3 Results

4.3.1 Water Analysis

The results of the water analyses are presented in Table 4.1

The electrical conductivity of the vlei water varies from 39500 μS/cm for sample CR5 to 313 μS/cm for sample CR26 which lies at the extreme south of the vlei system and is separated from the rest of the vlei by a berm. This area of the southern channel, south of the berm receives storm water runoff from the Paarden Eiland semi-industrial area. As the berm obstructs flow northwards, this region remains relatively full all year round. The vlei water samples may be divided into two groups based on their electrical conductivities, the EC of the two groups differing by approximately an order of magnitude. Samples CR1 to CR24 represent the higher EC samples and were taken prior to the winter rains; therefor, they represent evaporative

Table 4.1. Total analyses of vlei water samples

Water Analyses

Sample No	pH	ECuS/cm	DOC (PPM)	ALK (mmol/l)	Cl (ppm)	Cl (mol/l)	SO4 (ppm)	SO4 (mol/l)	Cl/SO4	Br (ppm)	NO3 (ppm)	NO3 (mol/l)
CR1	8.14	29600										0.000000
CR2	8.11	2830	24	4.56								0.000000
CR3	7.98	1082										0.000000
CR4	8.24	881	7	5.48								0.000000
CR5A	8.21	18780	5									0.000000
CR5	7.56	39500										0.000000
CR6	8.28	18720	7									0.000000
CR7												0.000000
CR8		1116	19	4.28	210.80	0.00595	57.84	0.000602	9.88	0.00	8.34	0.000151
CR9		776	12	3.16	103.10	0.00291	51.88	0.000541	5.37	0.00	6.65	0.000107
CR10		669	7	2.86	90.37	0.00256	86.04	0.000666	2.86	0.00	0.00	0.000000
CR11	7.33	863	18	1.80	110.23	0.00311	56.43	0.000577	5.39	0.00	12.14	0.000196
CR12	7.36	2170	1	3.80	544.01	0.01534	225.13	0.002344	6.56	0.00	67.89	0.001095
CR13	8.76	853	3	1.04	100.04	0.00282	72.70	0.000757	3.73	0.00	48.74	0.000786
CR14	8.74	15660	41	2.80	4598.05	0.12969	4284.73	0.044606	2.91	0.00	0.00	0.000000
CR15	7.36	331	9	1.80	38.15	0.00108	31.82	0.000331	3.25	0.00	2.87	0.000046
CR16	7.01	516	13	1.16	82.06	0.00232	79.25	0.000825	2.81	0.00	10.05	0.000162
CR17	8.62	15300	36	2.16	4861.66	0.13713	4553.12	0.047400	2.89	0.00	0.00	0.000000
CR18	6.86	15710	36	2.16	72.36	0.00204	103.60	0.001079	1.88	0.00	0.00	0.000000
CR19	8.54	16090	31	2.00	4316.33	0.12175	4221.47	0.043947	2.77	0.00	0.00	0.000000
CR20	3.16	4290	28	2.04	820.45	0.01750	1801.72	0.018757	0.93	0.00	0.00	0.000000
CR21	3.77	3900	2		901.06	0.01695	1625.70	0.016924	1.00	0.00	205.89	0.003321
CR22	8.53	13870	32	2.36	4107.75	0.11586	2247.36	0.023398	4.95	0.00	0.00	0.000000
CR23	8.70	13730	28	2.56	423.06	0.01193	2562.68	0.026678	0.45	0.00	0.00	0.000000
CR24	7.00	10240	16	3.76	3261.99	0.09201	947.89	0.009868	9.32	0.00	0.00	0.000000
CR25	7.28	1632	21	3.12	312.53	0.00882	197.43	0.002056	4.29	0.00	0.00	0.000000
CR26	7.23	313	3	1.16	85.81	0.00186	40.28	0.000419	4.43	0.00	4.27	0.000069
CR27	7.47	752	9		135.86	0.00383	94.32	0.000982	3.90	0.00	10.16	0.000164
CR28	7.29	621	2	1.56	115.96	0.00327	73.49	0.000765	4.28	0.00	8.39	0.000135
CR29	7.15	529	4	1.72	109.34	0.00308	88.33	0.000881	4.47	0.00	5.18	0.000084
CR30	7.07	906	6	2.24	170.86	0.00482	113.50	0.001182	4.08	0.00	5.42	0.000087
CR31	7.09	851	5	2.24	172.94	0.00486	118.03	0.001229	3.97	0.00	5.44	0.000088
CR32	7.08	866	1	2.40	189.07	0.00533	129.24	0.001345	3.96	0.00	9.08	0.000086
CR33	7.23	709	3	1.80	148.86	0.00420	112.84	0.001175	3.58	0.00	31.28	0.000504
CR34	7.28	871	3	1.88	142.72	0.00403	112.83	0.001176	3.42	0.00	34.86	0.000563
CR35	7.18	788	4	2.04	132.61	0.00374	105.39	0.001097	3.41	0.00	17.28	0.000279
CR36	7.08	5454	3	1.32	75.66	0.00213	54.31	0.000565	3.77	0.00	4.41	0.000071
CR37	7.03	321	0	1.04	50.71	0.00143	36.04	0.000396	3.61	0.00	3.84	0.000062
CR38	8.84	615	16	2.08	136.88	0.00382	13.85	0.000144	27.16	0.00	0.00	0.000000
CR39	7.18	1232	14	3.32	270.00	0.00762	87.54	0.001015	7.50	0.00	0.00	0.000000
CR40	7.43	1350	9	2.68	286.86	0.00809	169.40	0.001764	4.58	0.00	10.30	0.000166
CR41	7.08	840	8	2.06	158.98	0.00448	103.03	0.001073	4.18	0.00	0.00	0.000000
CR42	7.38	870	5	1.80	145.93	0.00412	114.71	0.001194	3.45	0.00	30.66	0.000495
CR43	8.35	628	2	1.40	130.93	0.00369	82.73	0.000853	5.85	0.00	0.00	0.000000
CR44	7.12	380	3	1.12	83.86	0.00180	43.18	0.000448	4.01	0.00	4.02	0.000065
CR45	7.10	617	8	2.16	165.10	0.00466	81.89	0.000856	4.87	0.00	9.12	0.000089
CR46	7.15	629	5	2.00		0.00000		0.000000	ERR			0.000000
CR47	7.13	624	8	2.84	223.67	0.00631	92.00	0.000956	8.58	3.80	0.00	0.000000
CR48	7.07	1289	10	2.92	254.54	0.00718	128.57	0.001307	5.49	0.00	8.42	0.000132
CR49	7.39	1043	15	2.76	236.00	0.00666	46.17	0.000501	13.28	3.88	4.87	0.000079
CR50	7.48	1253	9	0.00	209.54	0.00591	126.09	0.001312	4.50	0.00	0.00	0.000000
CR51	7.63	1435	8	2.84	281.44	0.00794	177.58	0.001848	4.29	0.00	9.58	0.000154
CR52	7.45	1411	11	2.88	272.56	0.00769	178.41	0.001857	4.14	0.00	9.88	0.000158
CR53	7.25	3120	8	3.36	536.51	0.01513	324.77	0.003381	4.48	0.00	0.00	0.000000
CR54	7.57	1467	13	2.84	280.15	0.00790	183.01	0.001905	4.15	0.00	8.22	0.000149
CR55	7.58	1458	8	2.76	278.30	0.00785	186.03	0.001937	4.05	0.00	12.48	0.000201
CR56	7.13	1451	9	3.08	288.98	0.00815	180.10	0.001879	4.12	0.00	9.17	0.000148
CR57	7.23	1517	8	3.14	285.83	0.00806	186.03	0.001937	4.16	0.00	11.83	0.000191
CR58	7.19	1456	10	2.96	285.80	0.00806	186.07	0.001937	4.16	0.00	7.06	0.000114
CR59	7.42	1497	9	3.04	277.72	0.00783	187.31	0.001950	4.02	0.00	8.59	0.000139
CR60	7.80	1569	7	3.20	314.28	0.00886	183.28	0.001906	4.65	0.00	8.61	0.000139
CR61	7.82	1051	3	3.32	172.33	0.00486	112.34	0.001169	4.16	0.00	24.83	0.000400
CR62	7.56	1568	8	3.28	314.54	0.00887	184.70	0.001923	4.61	5.62	7.41	0.000120
CR63	7.32	1450	13	2.92	277.50	0.00783	180.51	0.001878	4.17	0.00	13.57	0.000218
CR65	7.44	1564	9	2.90	305.56	0.00862	180.57	0.001984	4.34	0.00	10.06	0.000163
CR66	7.85	488	8	3.00	83.56	0.00236	39.28	0.000409	5.76	0.00	3.23	0.000052
CR67	7.56	1516	9	3.08	310.25	0.00875	191.59	0.001995	4.38	0.00	0.00	0.000000
CR68	7.02	980	10	2.82	171.24	0.00483	66.85	0.000717	6.74	0.00	9.43	0.000104
CR69	7.16	1479	17	3.16	293.03	0.00827	121.88	0.001267	6.52	0.00	9.82	0.000142
CR70	7.82	1562	10	3.08	308.78	0.00871	138.80	0.001446	6.02	0.00	9.48	0.000137
CR71	7.02	1480	13	3.56	310.40	0.00876	122.40	0.001274	6.87	0.00	0.00	0.000000
CR72	7.02	1585	16	4.12	309.14	0.00872	133.51	0.001390	6.27	0.00	9.16	0.000148

Sample No.	PO4(ppm)	Zn (ppm)	Pb(ppm)	Cd(ppm)	Fe(ppm)	Mg(ppm)	Mg(mol/l)	Ca(ppm)	Ca(mol/l)	Na(ppm)	Na(mol/l)	K (ppm)
CR1		0.464	0.085	0.053	2.330	853.00	0.035096	97.9	0.013622	5800.0	0.252266	597.0
CR2		0.090	0.007	0.010	1.120	61.80	0.002543	44.9	0.002443	529.0	0.023010	44.9
CR3		0.078	0.017	0.008	2.060	12.50	0.000514	179.0	0.001120	157.0	0.006829	11.2
CR4		0.028	0.038	0.021	0.359	345.00	0.014195	277.0	0.004466	1940.0	0.084365	119.0
CR5A		0.037	0.001	0.042	0.087	836.00	0.034396	474.0	0.006911	3880.0	0.168771	268.0
CR5		0.048	0.000	0.070	0.092	1830.00	0.075293	265.0	0.011826	7590.0	0.334497	603.0
CR6		0.025	0.012	0.030	0.127	750.00	0.030858		0.008612	3780.0	0.164421	279.0
CR7							0.000000		0.000000		0.000000	
CR8	0						0.000000	59.9	0.000000		0.000000	
CR9	0	0.023	0.017	0.009	1.970	9.55	0.000393	56.1	0.001495	86.0	0.003741	12.3
CR10	0	0.056	0.009	0.000	1.660	7.34	0.000302	37.7	0.001400	74.1	0.003223	11.2
CR11	0	0.378	0.038	0.005	2.210	2.52	0.000104	213.0	0.000941	96.2	0.004184	7.9
CR12	0	0.257	0.007	0.020	5.970	39.30	0.001617	47.2	0.005314	277.0	0.012049	18.3
CR13	0	0.150	0.026	0.008	0.203	6.31	0.000260	1020.0	0.001178	71.5	0.003110	10.2
CR14	0	0.328	0.032	0.064	1.490	959.00	0.039457	25.0	0.025449	2870.0	0.124838	361.0
CR15	0	0.046	0.018	0.000	1.150	0.42	0.000017	21.2	0.000624	48.3	0.002101	2.5
CR16	0	0.081	0.000	0.000	3.630	4.37	0.000180	815.9	0.000529	80.8	0.003515	9.0
CR17	0	0.623	0.070	0.017	1.542	566.10	0.023292	749.0	0.020356	2234.4	0.097192	267.4
CR18	0	0.265	0.025	0.026		622.00	0.025591	792.0	0.018688	2620.0	0.113964	352.0
CR19	0	0.166	0.042	0.033	0.802	661.00	0.027196	427.0	0.019780	2670.0	0.116139	360.0
CR20	0	3.360	0.035	0.033	32.800	146.00	0.006007	473.0	0.010654	417.0	0.018139	64.0
CR21	0	3.410	0.043	0.037	6.330	159.00	0.006542	636.0	0.011801	426.0	0.018617	65.4
CR22	0	0.029	0.022	0.025	0.275	478.00	0.019667	640.0	0.015868	2430.0	0.105699	271.0
CR23	0	0.053	0.000	0.030	1.070	500.00	0.020572	312.0	0.015968	2330.0	0.101349	253.0
CR24	0	0.068	0.011	0.018	1.450	350.00	0.014400	88.7	0.007784	2030.0	0.088300	164.0
CR25	0	0.004	0.000	0.016	0.959	27.50	0.001131	26.9	0.002213	104.0	0.004524	36.4
CR26	0	0.606	0.069	0.012	0.900	5.47	0.000225	53.1	0.000671	46.3	0.002014	4.8
CR27	0	0.159	0.022	0.014	0.305	16.20	0.000667	49.8	0.001325	92.9	0.004041	13.6
CR28	0	0.340	0.077	0.015	1.480	13.30	0.000547	41.5	0.001243	81.9	0.003562	10.4
CR29	0	0.167	0.030	0.011	0.348	9.20	0.000379	62.1	0.001035	78.5	0.003415	3.7
CR30	0	0.072	0.017	0.014	0.345	15.00	0.000617	67.6	0.001549	108.0	0.004696	7.9
CR31	0	0.078	0.018	0.010	0.404	15.60	0.000642	66.2	0.001692	108.0	0.004696	7.9
CR32	0	0.052	0.007	0.011	0.343	16.60	0.000683	65.0	0.001652	111.0	0.004826	8.9
CR33	0	0.260	0.073	0.012	1.180	3.80	0.000156	80.0	0.001622	96.3	0.004189	19.3
CR34	0	0.148	0.000	0.017	0.270	20.90	0.000860	60.0	0.001996	89.5	0.003893	17.9
CR35	0	0.217	0.003	0.010	0.204	12.50	0.000514	34.1	0.001497	94.3	0.004102	15.9
CR36	0	0.136	0.000	0.007	0.218	6.47	0.000266	25.5	0.000851	57.6	0.002505	5.1
CR37	0	0.204	0.042	0.012	0.344	4.78	0.000197	33.5	0.000836	36.7	0.001596	4.0
CR38	0	0.021	0.002	0.007	1.900	9.05	0.000372		0.000836	87.6	0.003810	17.0
CR39	0						0.000000	75.0	0.000000		0.000000	
CR40	0	0.020	0.016	0.010	0.956	23.30	0.000959	55.6	0.001671	105.0	0.004567	35.2
CR41	0	0.121	0.022	0.013	0.410	13.50	0.000555	65.4	0.001367	102.0	0.004437	7.0
CR42	0	0.238	0.036	0.014	0.480	14.70	0.000605	32.6	0.001632	97.6	0.004254	18.8
CR43	0	0.215	0.071	0.012	1.270	6.81	0.000280	26.0	0.000818	58.6	0.002549	5.5
CR44	0	0.087	0.000	0.011	0.176	5.36	0.000221	64.1	0.000649	42.6	0.001853	5.0
CR45	0	0.030	0.018	0.012	0.905	17.60	0.000724	63.0	0.001599	95.3	0.004145	13.2
CR46		0.060	0.000	0.009	0.326	17.00	0.000699	81.6	0.001572	95.2	0.004141	13.6
CR47	0	0.012	0.000	0.016	0.725	25.50	0.001049	86.8	0.002036	99.4	0.004324	19.9
CR48	0	0.057	0.002	0.015	0.856	30.40	0.001251	55.6	0.002166	87.2	0.003793	27.8
CR49	0	0.005	0.000	0.011	0.853	21.60	0.000889	88.5	0.001387	95.0	0.004132	24.5
CR50	0	0.029	0.000	0.016	1.030	31.00	0.001275	94.4	0.002206	85.2	0.003706	27.6
CR51	0	0.018	0.012	0.015	1.150	33.80	0.001392	95.2	0.002355	85.6	0.002853	31.1
CR52	0	0.014	0.000	0.014	1.000	31.80	0.001308	84.6	0.002375	76.8	0.003332	31.2
CR53	0	0.006	0.010	0.015	0.548	25.50	0.001049	102.0	0.002111	110.0	0.004785	37.4
CR54	0	0.016	0.007	0.015	1.030	36.10	0.001485	98.5	0.002545	68.4	0.002975	31.6
CR55	0	0.016	0.000	0.014	1.040	34.40	0.001415	105.0	0.002408	69.1	0.003006	31.3
CR56	0	0.016	0.001	0.017	0.752	36.50	0.001502	108.0	0.002620	65.7	0.002858	33.5
CR57	0	0.021	0.000	0.016	2.050	36.00	0.001481	99.9	0.002695	70.4	0.003062	34.5
CR58	0	0.013	0.000	0.016	0.599	34.90	0.001436	112.0	0.002493	64.6	0.002810	32.1
CR59	0	0.016	0.010	0.025	1.730	42.40	0.001744	106.0	0.002794	76.9	0.003432	31.0
CR60	0	0.012	0.000	0.020	0.649	36.00	0.001481	78.4	0.002645	44.7	0.001944	36.4
CR61	0	0.009	0.004	0.010	0.003	22.80	0.000938	101.0	0.001956	97.9	0.004258	36.5
CR62	0	0.024	0.000	0.019	1.210	34.10	0.001403		0.002520	51.8	0.002253	35.4
CR63	0						0.000000	102.0	0.000000		0.000000	
CR65	0	0.064	0.010	0.016	3.290	37.20	0.001531	34.2	0.002545	58.6	0.002462	35.6
CR66	0	0.117	0.011	0.011	0.139	8.66	0.000356	106.0	0.000853	63.0	0.002740	6.6
CR67	0	0.145	0.046	0.020	5.870	39.10	0.001609	71.7	0.002695	43.6	0.001896	37.3
CR68	0	0.018	0.015	0.015	1.330	22.70	0.000934	81.8	0.001789	99.3	0.004319	20.4
CR69	0	0.007	0.001	0.016	0.803	34.80	0.001432	86.4	0.002041	67.2	0.002923	32.7
CR70	0	0.001	0.013	0.015	0.129	35.70	0.001469	86.4	0.002131	34.2	0.001488	34.5
CR71	0	0.013	0.008	0.013	0.275	35.20	0.001448	115.0	0.002131	26.7	0.001161	36.5
CR72	0	0.011	0.018	0.022	0.466	44.40	0.001827		0.002869	57.6	0.002505	35.8

Sample No.	K(mol/l)	Al(ppm)	Cu(ppm)	% charge imb
CR1	0.015289	5.000	0.058	
CR2	0.001148	0.437	0.010	
CR3	0.000286	0.234	0.014	
CR4	0.003044	0.218	0.017	
CR5A	0.007386	0.150	0.008	
CR5	0.015423	0.186	0.005	
CR6	0.007136	0.182	0.010	
CR7	0.000000			
CR8	0.000000			
CR9	0.000315	0.106	0.003	-3.126
CR10	0.000266	0.242	0.007	1.845
CR11	0.000203	0.905	0.034	-0.924
CR12	0.000468	0.284	0.030	-0.726
CR13	0.000261	0.423	0.010	4.980
CR14	0.009745	2.530	0.043	-8.822
CR15	0.000083	0.406	0.009	-0.859
CR16	0.000230	0.167	0.013	2.540
CR17	0.005639	1.359	0.170	10.028
CR18	0.009003	0.961	0.022	-94.165
CR19	0.009208	1.140	0.024	-1.782
CR20	0.001637	7.370	0.059	2.835
CR21	0.001673	6.470	0.056	-0.210
CR22	0.006931	0.097	0.024	-5.343
CR23	0.006471	1.160	0.021	-45.472
CR24	0.004196	0.469	0.012	-8.462
CR25	0.000931	0.066	0.003	13.825
CR26	0.000123	0.432	0.007	0.235
CR27	0.000348	0.132	0.011	-15.578
CR28	0.000266	0.456	0.023	-5.850
CR29	0.000094	0.239	0.015	-0.070
CR30	0.000202	0.105	0.006	1.885
CR31	0.000203	0.179	0.006	0.860
CR32	0.000229	0.080	0.006	4.356
CR33	0.000494	0.647	0.013	5.954
CR34	0.000458	0.106	0.006	-4.823
CR35	0.000407	0.278	0.006	-0.164
CR36	0.000131	0.146	0.006	-1.656
CR37	0.000103	0.247	0.012	-0.079
CR38	0.000436	0.153	0.007	-3.012
CR39	0.000000			100.000
CR40	0.000900	0.119	0.006	14.231
CR41	0.000180	0.210	0.011	1.077
CR42	0.000481	0.281	0.014	0.305
CR43	0.000141	0.909	0.032	12.406
CR44	0.000127	0.228	0.006	2.666
CR45	0.000336	0.147	0.006	-1.169
CR46	0.000348	0.024	0.006	-83.748
CR47	0.000509	0.057	0.003	0.280
CR48	0.000711	0.160	0.002	8.838
CR49	0.000627	0.137	0.003	8.299
CR50	0.000706	0.063	0.004	-14.284
CR51	0.000795	0.063	0.004	14.111
CR52	0.000796	0.056	0.004	11.865
CR53	0.000957	0.086	0.003	35.378
CR54	0.000808	0.056	0.003	11.248
CR55	0.000801	0.052	0.003	13.025
CR56	0.000957	0.053	0.002	12.840
CR57	0.000662	0.087	0.004	11.359
CR58	0.000821	0.065	0.003	13.990
CR59	0.000793	0.036	0.003	6.162
CR60	0.000931	0.018	0.002	18.444
CR61	0.000934	0.028	0.004	1.525
CR62	0.000906	0.069	0.003	16.187
CR63	0.000000			100.000
CR65	0.000911	0.176	0.007	15.309
CR66	0.000175	0.161	0.021	7.973
CR67	0.000954	0.197	0.010	15.815
CR68	0.000622	0.071	0.003	-5.111
CR69	0.000636	0.073	0.003	14.229
CR70	0.000662	0.045	0.003	21.952
CR71	0.000934	0.093	0.003	23.227
CR72	0.000918	0.043	0.001	10.793

The relative standard deviations for Pb and Cd exceeded that which is considered acceptable given machine specification. Therefore apparent variations in Pb and Cd concentrations are insignificant.

Sample No.	K(mol/l)	Al(ppm)	Cu(ppm)	% charge imb
CR1	0.015288	5.000	0.058	
CR2	0.001148	0.437	0.010	
CR3	0.000288	0.234	0.014	
CR4	0.003044	0.216	0.017	
CR5A	0.007368	0.150	0.008	
CR5	0.015423	0.186	0.005	
CR6	0.007136	0.162	0.010	
CR7	0.000000			
CR8	0.000000			
CR9	0.000315	0.105	0.003	-3.128
CR10	0.000286	0.242	0.007	1.845
CR11	0.000203	0.906	0.034	-0.924
CR12	0.000488	0.264	0.030	-0.728
CR13	0.000261	0.423	0.010	4.960
CR14	0.009745	2.630	0.043	-8.822
CR15	0.000063	0.408	0.009	-0.858
CR16	0.000230	0.167	0.013	2.540
CR17	0.006639	1.358	0.170	10.026
CR18	0.009003	0.961	0.022	-84.185
CR19	0.009206	1.140	0.024	-1.782
CR20	0.001637	7.370	0.056	2.835
CR21	0.001673	6.470	0.056	-0.210
CR22	0.006931	0.097	0.024	-5.343
CR23	0.006471	1.180	0.021	-45.472
CR24	0.004196	0.469	0.012	-8.462
CR25	0.000931	0.069	0.003	13.825
CR26	0.000123	0.432	0.007	0.235
CR27	0.000348	0.132	0.011	-15.578
CR28	0.000266	0.456	0.023	-5.850
CR29	0.000064	0.239	0.015	-0.070
CR30	0.000202	0.105	0.005	1.885
CR31	0.000203	0.179	0.006	0.860
CR32	0.000229	0.080	0.006	4.366
CR33	0.000494	0.647	0.013	5.954
CR34	0.000458	0.106	0.006	-4.823
CR35	0.000407	0.278	0.008	-0.164
CR36	0.000131	0.148	0.009	-1.856
CR37	0.000103	0.247	0.012	-0.079
CR38	0.000435	0.153	0.007	-3.012
CR39	0.000000			100.000
CR40	0.000900	0.119	0.005	14.231
CR41	0.000180	0.210	0.011	1.077
CR42	0.000481	0.291	0.014	0.305
CR43	0.000141	0.909	0.032	12.406
CR44	0.000127	0.228	0.005	2.868
CR45	0.000336	0.147	0.008	-1.199
CR46	0.000348	0.024	0.006	-63.749
CR47	0.000509	0.067	0.003	0.280
CR48	0.000711	0.160	0.002	8.838
CR49	0.000627	0.137	0.003	6.299
CR50	0.000706	0.063	0.004	-14.294
CR51	0.000785	0.063	0.004	14.111
CR52	0.000798	0.056	0.004	11.886
CR53	0.000957	0.066	0.003	35.378
CR54	0.000808	0.056	0.003	11.248
CR55	0.000801	0.052	0.003	13.025
CR56	0.000857	0.053	0.002	12.840
CR57	0.000882	0.067	0.004	11.358
CR58	0.000621	0.055	0.003	13.880
CR59	0.000793	0.036	0.003	8.162
CR60	0.000931	0.018	0.002	18.444
CR61	0.000934	0.028	0.004	1.525
CR62	0.000906	0.069	0.003	19.187
CR63	0.000000			100.000
CR65	0.000911	0.176	0.007	15.309
CR66	0.000175	0.161	0.021	7.973
CR67	0.000954	0.187	0.010	15.915
CR68	0.000622	0.071	0.003	-5.111
CR69	0.000636	0.073	0.003	14.229
CR70	0.000682	0.045	0.003	21.852
CR71	0.000934	0.093	0.003	23.227
CR72	0.000918	0.043	0.001	10.793

The relative standard deviations for Pb and Cd exceeded that which is considered acceptable given machine specification. Therefore apparent variations in Pb and Cd concentrations are insignificant.

The wavelengths used for the elemental determination of the dissolved constituents in the vlei water, using ICP-AES.

Element	Wavelength (nm)
Zn	213.856
Pb	220.353
Cd	226.502
Fe	259.940
Mg	279.553
Al	308.215
Cu	324.754
Ca	393.367
Na	589.592
K	766.490

concentrates of the vlei water. The EC of the "low conductivity" samples is highly variable. Samples taken from the southern channel and stormwater inlet drains entering the southern channel from both the residential and semi-industrial areas (CR27 - CR48) appear to have a lower EC than those samples taken from the pans and the interconnecting channel where the water is circulating (CR48 - CR72, except for samples CR61 and CR66). It appears that the samples taken from perennial regions of the vlei system have a higher EC than those sampled from areas permanently submerged. A possible explanation for this observation is the dissolution of the thin layer of white salt/precipitate which was observed on the exposed sediments prior to their submergence. CR61 and CR66 were sampled from inlet drains from the residential and semi-industrial areas respectively. Sample CR61 has an EC comparable with that of the "bulk" vlei water while CR66 has a significantly lower EC (488 μS/cm).

The pH of the vlei water varies from 9.24 for sample CR4 taken from the channel to the north of the Northern pan just prior to the R27 and Boundary Rd intersection in Milnerton, to 6.53 for sample CR22 taken from the southern edge of the northern pan when the vlei was approximately half full (i.e. approximately half the surface area of the northern pan was submerged). For the majority of the vlei water samples, particularly those taken after the winter rains, the pH varies from 7.0 to 7.5. This coincides with the expected pH for low alkalinity river water (7.30, Dryssen and Wedborg, 1980) where mineral weathering processes and equilibrium with basic cations are responsible for neutralisation of the acidity of rain water brought about by the dissolution of CO_2.

The total alkalinity of the vlei water varies from 5.48 to 1.04 mmol/l. At a pH of between 7.00 and 7.50 the carbonate species present in solution is the HCO_3^- species (Stumm and Morgan, 1970). The total alkalinity of those samples taken from concentrated evaporation ponds is more variable than those sampled from the "bulk" vlei, due to mixing and homogenisation of the vlei water. The alkalinity is a measure of the buffering capacity of the vlei water. The formal definition of alkalinity is the following: "for solutions that contain no protolysis system other than that of aqueous

carbonate, alkalinity is a measure of the quantity of acid per litre required to attain a pH equal to that of a C_T-molar solution of $H_2CO_3^*$."(Stumm amd Morgan, 1970). Because the respective equivalence points for the determination of alkalinity represent the thresholds beyond which biological life is seriously impaired, the total alkalinity is a quick and convenient measure for estimating the maximum capacity of the water to neutralise acidity without posing a serious threat to the ecosystem (Stumm and Morgan, 1970).

The concentration of dissolved organic carbon in the vlei water varied considerably, from 41 ppm to 0 ppm. The highest concentrations of dissolved organic carbon where obtained for the "high EC" sample set, i.e. those samples taken from stagnant concentrated evaporation ponds where equilibration of the water with decaying organic matter associated with the sediments was attained. Dissolved organic carbon was determined in the water due to the fact that the affinity of dissolved organics for particularly Pb and Cu is believed to be exceptionally high (Lazerte *et al.*, 1989). Humic substances constitute a large proportion of dissolved organic matter in natural waters and are complex macromolecular phenolic carboxylic acids with a wide variety of surface functional groups, anionic in character and therefore capable of metal complexation (Duinker, 1980). The concentration of dissolved organic matter in the vlei far exceeds that of trace metals (Table 4.1), suggesting that the low concentrations of dissolved trace metals will be complexed with dissolved organic matter, and thus perhaps be unavailable for adsorption. Dissolved organic molecules are able to complex with metals by ion exchange, surface adsorption and chelation (Duinker, 1980). However, it appears that the solubility of Pb is controlled by either adsorption reactions (see previous chapter), or by the solubility of $PbCO_3$(s) as the addition of $PbNO_3$(s) to vlei water led to the precipitation of $PbCO_3$ as described in section 3.2.2.5. In order to assess the extent of dissolved organic matter complexation with Pb and Zn, all the equilibrium constants and stoichiometry for the possible reactions between Pb and Zn and all the surface functional groups must be known - clearly an impossibility.

Spearman rank correlation coefficients were calculated using Statgraphics version 6.0

on the Earth Sciences HP9000 computer in order to asses the degree of association of the dissolved organic carbon content and the concentration of trace metals in the vlei water. The results are presented in Appendix 11, and it is evident that there is no association of dissolved organic carbon with dissolved trace metal concentrations. This, however, does not indicate that trace metal - organic matter complexation is weak, but merely that those samples rich in organic carbon are not necessarily enriched also in trace metals. Due to the lack of information regarding metal-organic matter complexation and the low organic carbon concentration in the majority of the samples, as well as the control on Pb solubility exerted by $PbCO_3$ precipitation observed in experiment 4.2.2.5., organic carbon will be disregarded in further discussion on the speciation of trace metals in solution.

Analyses of major elements are presented in Table 4.1. The concentrations of the major elements are intermediate between those of standard sea water and river water (Dyrssen and Wedborg, 1980), a reflection of the brackish nature of the vlei. The low chloride to sulphate ratio (predominantly ranging between 3 and 7 compared to 19.3 for standard sea water (Dyrssen and Wedborg, 1980)) indicates that the vlei water does not merely represent sea water diluted with rain water and storm water runoff. The elevated sulphate concentration is the result of oxidation of abundant Fe and Mn sulphides in the sediments in the form of greigite and mackiniawite in contact with the vlei water. NO_3^- concentrations vary from 0 to 205 ppm. All samples with significantly elevated concentrations of NO_3^- (CR12, CR13, CR21, CR33, CR34 and CR61) represent stormwater from the Rugby-Milnerton residential area. The most probable source of the excess nitrate is fertiliser used in nearby residential gardens and sports fields. No bromide (whose association with Pb would indicate petrol and diesel as the source) was detected in the vlei water.
The dominant cations in the vlei water are in order of decreasing concentration: Na^+, Ca^{2+} and Mg^{2+} and K^+ in roughly equal concentrations.

The following trace metal concentrations in the vlei water are presented in Table 4.1: Zn, Pb, Cu, Cd, Fe and Al. However, the accuracy and precision of the Pb and Cd determinations are limited by the working detection limits of the method of analysis

as the high relative standard deviation values reported in Table 4.1 indicate. Therefore the discussion on trace metal concentrations in the vlei water will be limited to dissolved Zn. All the trace metal concentrations are elevated compared to average background concentrations in river water and sea water (see Table 4.1). These elevated concentrations must be interpreted with caution due to the fact that the water samples for cation analysis were acidified prior to filtration. Dissolution of, and desorption reactions from, particulate matter prior to filtration might therefore be a possible cause of the apparent elevated trace metal concentrations.

Discernible trends regarding the concentrations of trace metals are evident despite the high degree of uncertainty. Concentrations of Zn in samples taken from concentrated evaporation ponds prior to the winter rains are elevated by more than an order of magnitude compared to the rest of the sample set, and there is a noticeable decrease in the Zn content of the vlei water moving in a northerly direction through the vlei system. Sample CR1 taken from an evaporation pond situated in the interconnecting channel between the northern and the southern pan is particularly concentrated and contains 464 μg/l Zn, more than an order of magnitude greater than the average background value presented in Table 4.2, however, significantly lower than the recommended guideline value for drinking water of 5.0 mg/l (WHO, 1984). Samples CR20 and CR21 were both taken from stagnant pools in which rusting corrugated iron was found. These samples have exceptionally elevated concentrations of Zn, Cd and Fe (3.36 and 3.41 ppm Zn; 32.8 and 8.33 ppm Fe and 33 and 37 μg/l Cd respectively). The high concentrations are undoubtedly the result of acidification and dissolution of particulate matter from the observed corrugated iron and indicate a possible source of these trace metals in the vlei water. CR26 is sampled from the southern tip of the vlei system, south of the berm at an inlet from the semi-industrial area and contains high concentrations of Zn in comparison to the rest of the sample set. The sample taken from the inlet from Paarden-Eiland just south of the northern pan (CR66) contains Zn in excess of those from both pans, but lower than those from the storm water inlet drains from the residential area in the southern channel (CR27, CR28 and CR33).

Table 4.2. Background concentrations of metals in sea water and fresh water. Values taken from Forstner and Wittman (1979).

Metal	sea water (μg/l)	fresh water (μg/l)
Lead	0.005 - 0.015	0.2
Zinc	0.01	10.0
Copper	0.1 - 0.04	1.8
Cadmium	0.01	0.07
Iron	1.30	<30
Aluminium	1.0	<30

The above discussion suggests that Pb and Zn are entering the vlei in the dissolved form. However, the source is diffuse and not necessarily confined to stormwater and effluent drains from Paarden-Eiland. Dissolved Zn is entering the vlei via storm water drains from the residential area, and via two storm water drains from the industrial area, one situated at the extreme south of the vlei system, the other between the southern and the northern pans. Samples taken from the channels and from storm water drains have higher trace metal concentrations than those sampled from the pans, possibly due to the fact that sediment-water equilibrium is not attained in the deeper channels in contrast to the shallow pans. The results of the analyses indicate that the Zn content of the vlei water in the northern pan and the outlet channel into the Milnerton Lagoon is elevated compared to the average background concentration (37μg/l). However, dilution on entering the lagoon would immediately reduce the elevated Zn concentrations to background values. Complete removal of Zn is not achieved by the sediments. However, the progressive decrease in dissolved Zn moving in a northerly direction through the vlei system suggests that the sediments in the vlei are efficient removers of trace metals.

4.3.2. Results of the experiment to determine the solubility of $PbCO_3$.

The results of this experiment are shown in Figure 4.1 with further data appearing in Appendix 12.

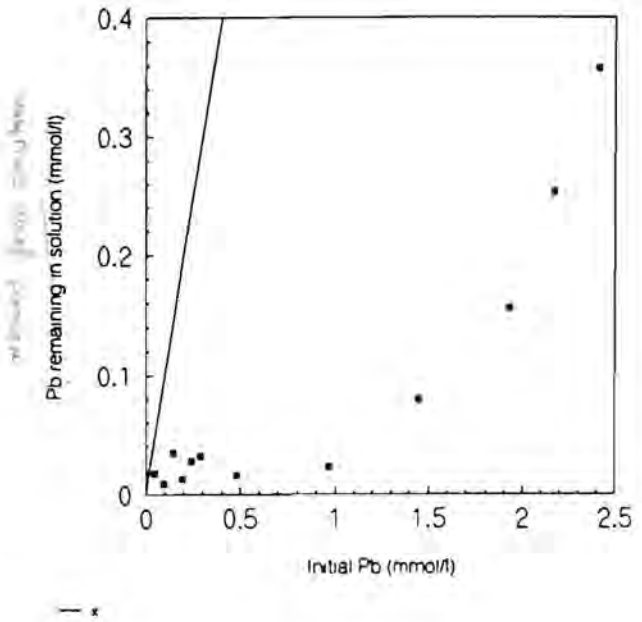

Figure 4.1. Experimentally determined solubility of $PbCO_3$ in vlei water with an alkalinity of approximately 3.0 mmol/l. The solid line represents complete removal of Pb from solution.

$PbCO_3$ is the most sparingly soluble Pb solid (K_{sp} = $1*10^{-13}$, solubility = 0.00011[20] g per 100 cc, (Weast, 1975)) and thus considering the significant carbonate content of the vlei water (total alkalinity approximately 3.0mmol/l), formation of $PbCO_3$(s) would be expected to remove Pb from solution. However, the results of the sequential extraction procedure carried out by Board (1993) and Farmer (1993) revealed that only a maximum of 8.5 % of the total Pb in the sediments is associated with carbonate phases. Figure 4.1 indicates that substantial Pb is removed from solution by precipitation of $PbCO_3$. $PbCO_3$ solubility appears to increase sharply at initial Pb concentrations exceeding 1mmol/l. However, concentrations of Pb exceeding 1mmol/l are unlikely to be introduced into the vlei. Introduction of 0.0483 mmol/l Pb (which corresponds to 10 ppm Pb) into vlei water results in the removal

of 0.0304 mmol/l Pb leaving 0.0179 mmol/l Pb in solution. The concentrations of Pb remaining in solution after carbonate precipitation far exceed both the concentrations of dissolved Pb in the vlei water and at equilibrium with the sediments in the supernatant of the adsorption experiments. These results, when compared with those of the adsorption experiments in chapter 3, indicate that Pb is more efficiently removed by adsorption in the sediments than by $PbCO_3$ precipitation. Thus $PbCO_3$ solubility is unlikely control the solubility of Pb in the vlei. A proportion of the Pb introduced into the vlei system will initially be removed by precipitation of $PbCO_3$ prior to contact with the sediments. However, adsorption reactions probably ultimately control Pb solubility.

4.3.3 Chemical speciation of the vlei water

Determination of the speciation of dissolved ions is a determination of the tendency for the ions in solution to complex with each other to form dissolved chemical species, and is based on experimentally determined stability constants for each complexation reaction under set environmental conditions. The chemical behaviour of a metal, i.e. its speciation and the reactions involved in the transformation of species, not its total concentration in water is the main factor determining its effect on the environment (Forstner and Wittman, 1979). Knowledge of whether the metal is present as a complexed species or a simple free ion, the charge of the species and the size of the metal species are important in determining the potential of that metal to be adsorbed and the bioavailability of the metal species (Forstner and Wittman, 1979). Here the speciation of the dissolved ions in the vlei water were calculated using the MINTEQA2 computer speciation programme. Knowledge of the speciation of the dissolved Pb and Zn in the vlei water, as opposed to the artificially prepared Pb and Zn nitrate solutions used in the adsorption experiments, highlights differences between laboratory and real conditions which affect the metal's potential for adsorption. Differences in the speciation of Pb and Zn will determine differences in the behaviour of these two metals with regard to adsorption in the vlei. The speciation of a "high salinity" and a "low salinity" sample are presented in Table 4.3.

The speciation information indicates that the majority of the Pb in solution is complexed to carbonate ions. Thus the chemistry of solvated Pb is very strongly influenced by reaction with carbonate ions, and the relative activities of these two ions in solution will influence the degree to which carbonate - Pb complexation occurs. At very low Pb activities, eg in the above two examples, the activity of Pb ions in solution is far exceeded by CO_3 ions resulting in complexation of a single Pb^{2+} ion with two CO_3^{2-} ions and the formation of the $Pb(CO_3)_2^{2-}$ species.

The majority of Zn in solution is in the form of the uncharged zinc hydroxide species. The information presented in Table 4.3 has important consequences regarding adsorption of these dissolved species. Most of the dissolved Pb and Zn are present as uncharged species in solution and a significant proportion, particularly of the Pb,

are present as negatively charged species. This differs remarkably from experimental conditions where the Pb and Zn were present purely as free divalent cations. Thus adsorption in the vlei system, unlike that in the experimental systems, must be specific in nature, involving covalent bonds and the surface complexation is independent of electrostatic interaction.

Table 4.3. Speciation of Pb and Zn in a high salinity and a low salinity sample in the vlei water.

High S.	log Act.	% ions	Low S.	log Act.	% ions
Total Pb	-10.55		Tot. Pb	-11.32	
$Pb(CO_3)_2^{2-}$	-7.73	44.7	$Pb(CO_3)_2^{2-}$	-7.28	47.1
$PbCO_3(aq)$	-7.22	36.4	$PbCO_3(aq)$	-7.38	24.0
$Pb(OH)_2(aq)$	-7.70	11.9	$Pb(OH)_2(aq)$	-7.48	19.0
$Pb(OH)^+$	-8.27	4.7	$Pb(OH)^+$	-8.55	1.8
$Pb(OH)_3^-$	-8.66	1.9	$Pb(OH)_3^-$	-7.94	7.4
$Zn(OH)_2(aq)$	-5.39	75.1	$Zn(OH)_2(aq)$	-5.54	79.0
$Zn(CO_3)_2^{2-}$	-6.64	16.6	$Zn(CO_3)^{2-}$	-6.57	11.5
$Zn(OH)_3^-$	-6.91	3.4	$Zn(OH)_3^-$	-6.56	8.4
ZnOHCl(aq)	-6.98	1.9			
$ZnCO_3(aq)$	-7.07	1.6			
$ZnOH^+$	-7.43	1.0			
Total Zn	-8.46		Total Zn	-9.60	

Figure 4.2 illustrates the redox equilibrium for the Pb-H_2O-CO_2 system where $Pb_T = 10^{-4}$ and $C_T = 10^{-2}$. Figure 4.2 indicates that at the pH and pE conditions

prevailing in the vlei, the precipitation of $PbCO_3$ will determine the concentration of dissolved Pb available for adsorption. The solubility of $PbCO_3$ depends upon the pH of the system and on the activities of the precipitating phase and Pb^{2+}. An influx of Pb and Zn into the vlei, given that the vlei is in equilibrium with atmospheric CO_2 and calcareous sediments, would thus result in the precipitation of Pb and Zn carbonate solids and equilibrium for the reactions of formation of Pb and Zn carbonate would be attained and control the amount of metal species remaining in solution. The above discussion regarding Pb speciation and the results of experiment 3.3.2 indicate that initially it is carbonate precipitation which determines the solubility of Pb in the vlei, after which, once equilibration with the sediments is achieved, and Pb is removed from solution by adsorption onto sediment particulate matter.

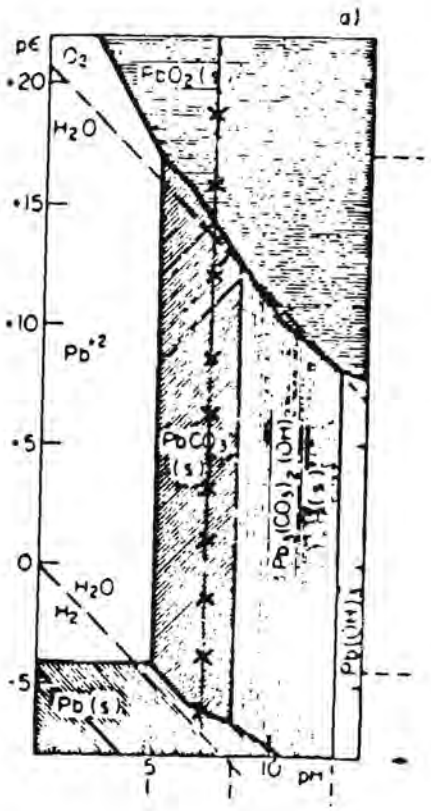

Figure 4.2. Redox equilibrium for the Pb-H_2O-CO_2 system, where $Pb_T = 10^{-4}$ and $C_T = 10^{-2}$. The crossed line indicates the pH of the vlei water, after Stumm and Morgan (1970).

The chemistry of solvated Zn is strongly affected by the formation of Zn hydroxides as well as Zn carbonates. The maximum total concentration of Zn that can be maintained in a carbonate bearing water ($C_T = 10^{-3}M$) as a function of pH, without becoming saturated with respect to zinc carbonate, hydrozincite or amorphous $Zn(OH)_2$ is illustrated in Figure 4.3 (Stumm and Morgan, 1970). Figure 4.3 is calculated on the basis of the following equations expressing the solubility of $ZnCO_3(s)$, hydrozincite and $Zn(OH)_2(s)$ (Stumm and Morgan, 1970):

$Zn(OH)_2(am) + 2H^+ = Zn^{2+} + 2H_2O$ $\quad \log K = 12.7$

$ZnCO_3(s) + 2H^+ = Zn^{2+} + H_2CO_3^*$ $\quad \log k = 6.7$

$Zn(OH)_{1.2}(CO_3)_{0.4}(s) + 2H^+ = Zn^{2+} + 0.4H_2CO_3^* + 1.2H_2O$ $\quad \log K = 6.7$

It is evident from Figure 4.3 that at pH's encountered in the vlei water, assuming that the water in Zoar Vlei is in equilibrium with atmospheric CO_2, the solubility of $ZnCO_3$ controls the maximum concentration of dissolved Zn in the vlei water available for adsorption by the sediments. At an approximately neutral pH, the maximum concentration of dissolved Zn is approximately $1*10^{-4}$ mol/l which corresponds to 6.35ppm. Thus the Zn in the vlei water is undersaturated with respect to $ZnCO_3(s)$. This indicates that Zn is being removed from solution by processes other than precipitation of zinc carbonate, hydrozincite and zinc hydroxide.

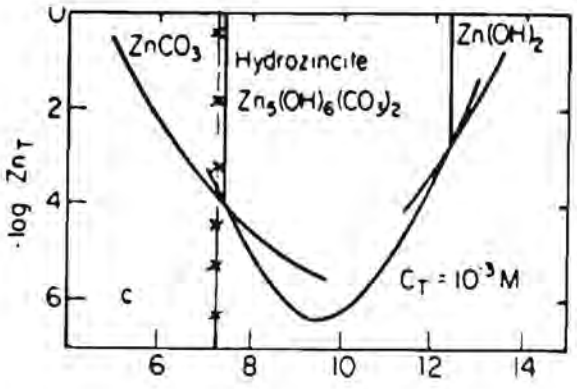

Figure 4.3. The solubility of Zn in a carbonate bearing water ($C_T = 10^{-3}$) as a function of pH. The crossed line indicates the pH of the vlei water, after Stumm and Morgan (1970).

4.4. Conclusions

The following conclusions can be drawn from the above discussion:

1. Concentrations of dissolved Zn are elevated in the vlei water compared to natural background values, however, are significantly lower than recommended guidelines for drinking water. As yet Zn poses no threat to the ecosystem. Zn appears to be entering the vlei via stormwater drains from both the industrial and residential areas.
2. Dissolved Zn concentrations decrease northward through the vlei system, but are still elevated at the outfow into the Milnerton Lagoon.
3. During summer evaporation results in concentrations of Zn in evaporation ponds more than an order of magnitude greater than average background values.
4. Due to the considerable carbonate content of the vlei water resulting from equilibrium with atmospheric CO_2 and the calcareous sediments, the majority of the Pb in the vlei water is complexed with the carbonate ligand resulting in the formation of the $Pb(CO_3)_2^{2-}$ and the $PbCO_3(aq)$ species. The majority of the Zn is present as $Zn(OH)_2(aq)$. Therefor, most of the Pb and Zn species are present as either neutral or negatively charged complexes. This indicates that adsorption must be specific in nature, not reliant on the electrostatic attraction between adsorbate and the surface functional group.
5. The solubility of Pb and Zn on entering the vlei in the dissolved form is initially controlled by precipitation of Pb and Zn carbonate. However, once equilibrium with the sediments is achieved adsorption controls trace metal solubility.

CHAPTER 5

Conclusions

The results of this investigation indicate that the solubility of Pb and Zn in Zoar Vlei is ultimately controlled by adsorption reactions with the sediments. This is evident from the high trace metal contents of the sediments and the approximate equivalence of the dissolved Pb and Zn concentrations in the vlei water and the supernatants produced in the adsorption experiments at low adsorbate concentrations. Both Pb and Zn concentrations in the vlei water are elevated compared to natural background concentrations. However, the detection limits of the analytical method used for the analyses are unacceptable with regards to Pb analysis. The fact that Zn concentrations after adsorption, as determined in the adsorption experiments, are equivalent to those found in the vlei water, and are elevated compared to natural background levels is an indication that the Zn adsorbing capacity of the sediments is approaching saturation with adsorbed Zn. This, coupled with the fact that Pb adsorption displaces Zn from adsorption sites, indicates that it is Zn that poses the greatest threat to the ecosystem. The sediments are, therefor, not capable of removing all the Zn entering the vlei, and elevated concentrations of Zn are thus being flushed out into the Milnerton Lagoon where the high concentrations are immediately eliminated by dilution with sea water.

The adsorption of Pb and Zn by the sediments is largely irreversible, except under acidified conditions where significant Zn is released. Thus the sediments appear to provide a permanent storage facility for Pb and acidification of the vlei poses the greatest threat to the ecosystem with regards to Zn toxicity.

The adsorption experiments were carried out on oxidised sediment samples using Pb and Zn nitrate solutions (where Pb and Zn are present as the free divalent cation), very different from the conditions prevailing in the vlei where Pb is predominantly present as the $Pb(CO_3)_2^{-}$ and $PbCO_3(aq)$ species and Zn as the $Zn(OH)_2(aq)$ species, and the sediments are highly reducing and contain abundant Fe and Mn sulphides. The oxidised nature of the sediment used in the adsorption experiments represents

the conditions under which minimum adsorption of trace metals is likely to occur and thus represents a worst case scenario for the adsorptive capacity of the sediments. Sulphides are considered to be excellent scavengers of trace metals (Jean and Bancroft, 1986) and increases in dissolved Pb, Cu and Ni have been reported subsequent to dredging as a result of oxidative remobilisation of the metals (Hall, 1988). The differences in the speciation of dissolved Pb and Zn under real and experimental conditions and the influence of speciation on adsorption requires investigation. However, the high trace metal contents of the sediments and the trace metal concentrations comparable with equilibrium concentrations in the adsorption experiments suggest that adsorption is not hindered by the presence of carbonate and hydroxy Pb and Zn species.

Recommendations for further work

Based on the findings of this report, the following recommendations for further work can be made:

1. Accurate determination of Pb and Cd concentrations in the vlei water are required.
2. The influx of dissolved Pb and Zn into the vlei via the storm water drains must be monitored, in order to determine the specific source of the metals, and to allow determination of the rate of accumulation of trace metals in the vlei system.
3. Investigation of sorption of trace metals by reduced sediment more accurately depicting the conditions in the vlei is required, i.e. sorption of trace metals by sulphide phases requires investigation.
4. The composition and speciation of dissolved components in the sediment pore water should be investigated, in order to obtain a better understanding of the processes occurring at the sediment-water interface, which control trace metal solubility in the vlei water.
5. The toxicity of Pb and Zn with respect to the flora and fauna in Zoar Vlei requires investigation, in order to identify the present and potential effect of elevated concentrations of these metals on the ecosystem.

Acknowledgements

I would like to thank Prof. J.P. Willis and Dr. M.V. Fey for supervising the project, Mr P. Sieas and Mrs. A. Upton for their help in the laboratory and Prof. R. Loewenthal and the Department of Civil Engineering for the use of the organic carbon analyser. Furthermore I am grateful to Ms M. Mckay of the Department of Chemistry for performing the elemental analyses using ICP-AES and a draughtsperson of Ninham Shand for kindly draughting maps 2 and 3.

References

Arafat, N. and Jerome, O.N. (1986). Simulated mobilisation of metals from sediments in response to lake acidification. Water, Air and Soil Pollution, 31, 991-998.

Balistrieri, L.S., Murray, J.W. and Paul, B. (1992). The biogeochemical cycling of trace metals in the water column of Lake Sammamish, Washington: Response to seasonally anoxic conditions. Limnology and Oceanography, 37(3) 529-548.

Balistrieri, L.S. and Murray, J.W. (1986). The surface chemistry of sediments from the Panama Basin: The influence of Mn oxides on metal adsorption. Geochimica et Cosmochimica Acta, 50 2235-2243.

Board, W.S. (1993). An assessment of heavy metal pollution in Zoar Vlei, Cape Peninsula, with specific reference to Zn, Cu, Pb and As. Unpublished Hons. Project. Faculty of Geological Sciences of the University of Cape Town.

Borchardt, G. (1989). Smectites. in minerals in soil environments. Soil Science Society of America. Madison pp 675-718. (Editors: Dixon, J.B. and Weed, S.B.).

Coetzee, P.P. (1993). Determination and speciation of heavy metals in sediments of the Hartbeespoort Dam by sequential chemical extraction. Water SA, 19(4) 291-300.

Di Toro, D.M., Mahony, J.D., Kirchgraber, P.R., O'Bryne, A.L., Pasquale, L.R. and Piccirilli, D.C. (1986). Effects of non-reversibility, particle concentration, and ionic strength on heavy metal sorption. Environmental Science and Technology, 20 55-61.

Dixon, J.B. (1989). Kaolin and serpentine group minerals. in minerals in soil environments. Soil Science Society of America. Madison pp 468-519. (Editors: Dixon, J.B. and Weed, S.B).

Drees, L.R., Wilding, L.P., Smeck, N.E. and Senkayi, A.I. (1989). Silica in soils: Quartz and disordered silica polymorphs. in Minerals in soil environments. Soil

Science Society of America. Madison. pp 914-965. (Editors: Dixon, J.B. and Weed, S.B.).

Dryssen, D. and Wedborg, M. (1980). Major and minor elements, chemical speciation in estuarine waters. In Olausson, E. and Cato, I. Chemistry and biogeochemistry of estuaries. John Wiley and Sons, New York pp71-120.

Duinker, J.C. (1980). Suspended matter in estuaries: adsorption and desorption processes. In Olausson, E. and Cato, I. Chemistry and biogeochemistry of estuaries. John Wiley and Sons, New York pp121-152.

Fanning, D.S., Keramidas, V.Z., and El-desoky, M.A. (1989). Micas. in minerals in soil environments. Soil Science Society of America. Madison. pp 552-624. (Editors: Dixon, J.B. and Weed, S.B.).

Farmer, (1993). An assessment of heavy metal pollution in Zoar Vlei, Cape Peninsula, with specific reference to Zn, Cu, Pb and As. Unpublished Hons. Project. Faculty of Geological Sciences of the University of Cape Town.

Farrah, H., Hatton, D. and Pickering, W.F. (1980). The affinity of metal ions for clay surfaces. Chemical Geology, 28 55-68.

Filipek, L.H. and Owen, R.B. (1978). Analysis of heavy metal distributions among different mineralogical states in sediments. Canadian Journal of Spectroscopy, 23(2) 31-35.

Forstner, U. (1987). Sediment associated contaminants - an overview of scientific bases for developing remedial options. Hydrobiologia, 149 221-246.

Forstner, U. and Wittman, G.T.W. (1979). Metal pollution in the aquatic environment. Springer-Verlag, Berlin-Heidelberg-New York 486pp.

Frenet, M. (1981). The distribution of mercury, cadmium and lead between water and suspended matter in the Loire Estuary as a function of the hydrological regime. Water Research, 15 1343-1350.

Hall, A.J. (1981). National Geographic Atlas of the World. National Geographic Society, Washington D.C.

Hall, L.A. (1988). The effects of dredging and reclamation on metal levels in water and sediments from an estuarine environment off Trinidad, West Indies.Environmental Pollution, 65 189-207.

Hart, B.T. (1982). Uptake of trace metals by sediments and suspended particulates: a review. Hydrobiologia, 91 299-313.

Hartnady, C.J.H. and Rogers, J. (1990). The scenery and geology of the Cape penninsula. Guidebook Geocongress '90 Geological Society South Africa, M1: 1-67.

Houba, C., Remacle, J., Dubois, D. and Thorez, J. (1983). Factors effecting the concentrations of cadmium, zinc, copper and lead in the sediments of the Vesdre River. Water Research, 17(10) 1281-1286.

Jean, G.E. and Bancroft, G.M. (1986). Heavy metal adsorption by sulphide mineral surfaces. Geochimica Cosmochimica Acta, 50 1455-1463.

Karlsson, S., Allard, B. and Hakansson, K. (1988). Chemical characterisation of stream-bed sediments receiving high loadings of acid mine effluents. Chemical Geology, 67 1-15.

Lazerte, B., Evans, D. and Grauds, P. (1989). Deposition and transport of trace metals in an acidified catchment of Central Ontario. The Science of the Total Environment, 87/88 209-221.

Masterton, W.L., Slowinski, E.J. and Stanitski, C.L. (1986). Chemical Principles with Qualitative Analysis. Suanders College Publishing, New York 1072pp.

Mc Kenzie, R.M. (1989). Manganese oxides and hydroxides. in Minerals in soil environments. Soil Science Society of America. Madison. pp 439-461. (Editors: Dixon, J.B. and Weed, S.B.).

Millward, G.E. and Moore, R.M. (1982). The adsorption of Cu, Mn and Zn by iron oxyhydroxide in model estuarine solutions. Water Research, 16 981-985.

Mott, C.J.B. (1989). The inorganic components of the soil. in Russells soil conditions and plant growth. Longman Scientific and Technical. New York pp 213-238. (Editor: Wild, A.).

Non-affiliated Soil Analysis Work Committee (1990). Handbook of standard soil testing methods for advisory purposes. Soil Science Society of South Africa pp34/1-34/2.

Pardo, F., Barrado, E., Perez, L. and Vega, M. (1990). Determination and speciation of heavy metals in sediments of the Pisuerga River. Water Research, 24(3) 373-379.

Panutrakul,S. and Baeyens, W. (1991). Behaviour of heavy metals in a mud flat of the Scheldt Estuary, Belgium. Marine Pollution Bulletin, 22(3) 128-134.

Rapin, F., Tessier, A., Campbell, P.G.C. and Carigan, R. (1986). Potential artifacts in the determination of metal partitioning in sediments by a sequential extraction procedure. Environmental Science and Technology, 20 836-840.

Salim, R. (1983). Adsorption of lead on the suspended particles of river water. Water Research, 17(4) 423-429.

Salomons, W., de Rooij, N.M, Kerdijk, H. and Bril, J. (1987). Sediments as a source

for contaminants? Hyrobiologia, 149 13-30.

Schwertmann, U. and Taylor, R.M. (1989). Iron Oxides. in Minerals in Soil Environments. Soil Science Society of America. Madison. pp 380-427. (Editors: Dixon, J.B. and Weed, S.B.).

Sinex, S.A. and Helz, G.R. (1982). Entrapment of zinc and other trace elements in a rapidly flushed industrial harbour. Environmental Science and Technology, 16 820-825.

Sposito, G. (1989). The chemistry of soils. Oxford University Press. New York pp262.

Stauffer, R.E. (1986). Cycling of manganese and iron in Lake Mendoto, Wisconson. Environmental Science and Technology, 20(5) 449-463.

Stumm, W. and Morgan, J.J. (1970). Aqutic chemistry: An introduction emphasising chemical equilibria in natural waters. John Wiley and Sons. New York pp563.

Tessier, S., Campbell, P.G.C. and Bisson, M. (1979). Sequential extraction procedure for the speciation of particulate trace metals. Analytical Chemistry, 51, 844-851.

Weast, R.C. (1975). Handbook of chemistry and physics. CRC Press, Ohio.

World Health Organisation (1984). Guidelines for drinking water quality. Geneva. pp 79.

Young, L.B. and Harvey, H.H. (1992). Geochemistry of Mn and Fe in lake sediments in relation to lake acidity. Limnology and Oceanography, 37(3) 603-613.

APPENDICES

APPENDIX 1

Pb, Zn, Cu sediment concentrations by XRF spectroscopy

% Organic Carbon determined by wet oxidation (Walkely Black)

Sample No.	Pb(ppm)	Zn(ppm)	Cu(ppm)	% org C
ZV1A	50.91	271.46	14.98	1.9
ZV1B	189.24	1011.99	64.18	0.93
ZV2A	149.46	795.52	50.93	2.92
ZV3A	196.89	1134.64	66.6	4.04
ZV4A	193.6	1105.64	61.27	3.51
ZV5A	143.76	778.28	49.73	2.91
ZV6A	199.2	1090.3	62.52	4.04
ZV7A	71.53	380.65	27.48	1.76
ZV9A	151.35	801.37	49.3	3.59
ZV10A	195.46	1172.49	64.11	1.2
ZV11A	183.51	1183.06	61.82	4.01
ZV12A	198.62	1143.17	67.25	2.59
ZV13A	231.58	1696.58	80.97	3.6
ZV14A	261.62	2179.95	94.04	4.99
ZV15A	266.06	1952.91	90.72	5.65
ZV16A	266.06	2270.91	83.82	4.45
ZV17A	193.78	1298.4	68.99	4.2
ZV18A	152.26	839.43	55.55	4.13
ZV19A	185.92	1237.09	59.25	3.66
ZV20A	196.75	1121.97	62.79	3.98
ZV21A	111.92	567.72	38.23	2.41
zvc2a	268	3501	86	6.47
zvc2b1	249	2987	77	3.62
zvc3a	89	472	33	1.55
zvc3b	27	103	9.6	0.54
zvc4a	196	948	60	2.89
zvc4b	61	272	19	0.8
zvc5b	36	172	14	0.54
zvc6a	326	1184	107	7.72
zvc6b	109	519	43	4.7
zvc7	70	157	28	1.25
zv8a	151.12	890.65	48.79	
zvc2b2	234	2528	74	
zvc5a	149	794	51	

Data taken from Board (1993) and Farmer (1993)

Sample No.	Pb(ppm)	Zn(ppm)	Cu(ppm)
a2s1	191	1614	71
a3s1	472	2980	200
a3s2	31	102	18
a4s1	276	173	11
a4s2	72	65	9.6
a4s3	80	83	14
a5s1	97	178	24
a5s2	83	122	11
a5s3	82	149	18
a5s4	275	519	63
a6s1	102	194	35
a6s2	86	125	17
a6s3	190	223	34
a7s1	16	30	8.9
a8s1	41	593	18
a9s1	312	2816	107
a9s2	280	2293	101
a9s3	282	2497	101
a9s4	78	1272	29
a9s5	25	158	19
b10s1	73	460	24
b10s2	41	91	11
b10s3(1)	11	22	14
b10s3(2)	8.9	17	7.7
b11s1	202	1312	72
b11s2	112	375	48
b11s3	30	82	17
b11s4	5.9	13	6.2
b11s5	10	20	7.9
b12s1	41	211	15
b12s2	37	123	15
b12s3	7.9	14	6.2
b13s1	136	816	48
b13s2	154	879	49
b13s3	21	80	12
b13s4	4.1	7.8	5.3
b13s5	17	29	9.9
b14s1	141	700	43
b14s2a	26	50	15
b14s2b	26	56	16
b15s1	20	60	8.6
b15s2a	6	11	5.2
b15s2b	4.9	8.8	5.2
b16s1	224	1057	72
b16s2	32	67	20
b1s1	232	2181	83
b1s2	233	2190	78
b1s3	95	353	35
b1s4	53	109	19
b2as1	262	2445	85
b2as2	270	2549	89
b2as3	333	5183	108
b2as4	154	671	56
b2bs1	261	2495	86
b2bs2	167	1011	26
b2bs3	26	58	11
b3s1	357	3830	104
b3s2a	83	509	26
b3s2b	60	211	21
b4s1	160	1474	56
b4s2	34	102	15
b4s3	22	23	7.1
b5s1	126	753	38
b5s2	47	165	20
b5s3	171	1025	67
b6s1	248	2441	71
b6s2	286	3059	81
b6s3	130	445	40
b6s4	58	168	22
b7s1	202	1712	65
b7s2	87	477	26
b7s3a	8.4	18	5.9
b7s3b	6.9	19	6.1
b8s1	156	961	48
b8s2	58	343	21
b8s3	11	27	6.2
b8s4	4.9	15	4.1
b9s2	309	1632	83
b9s3	19	33	11
c1s1	359	871	106
c1s2	31	83	11
c1s3	7.8	13	5.7
d10s1	99	303	36
d10s2	16	29	5.9
d10s3	15	30	10
d1s1	420	471	128
d1s2	17	64	15
d1s3	2.5	5.9	3.8
d1s4	6.3	12	6.3
d2s1	22	77	12
d2s2	37	80	18
d3s1	38	110	15
d3s2	43	75	18
d3s3	41	75	5.4
d4s1	219	1087	70
d4s2	38	99	18
d4s3	5.1	10	5.5
d5s1	21	63	11
d5s2	92	450	40
d6s1	111	430	49
d7s1	43	103	21
d8s1	23	74	15
d9s1	26	111	20
e1s1	110	270	43
e2s1	178	51	13
f1s1	128	243	13
f2s1	28	50	11
f4s2	138	99	23
f3s2	7.3	10	3.3

APPENDIX 2

Diffractograms for XRD analyses of sediment samples ZVC6A and ZVC7A.

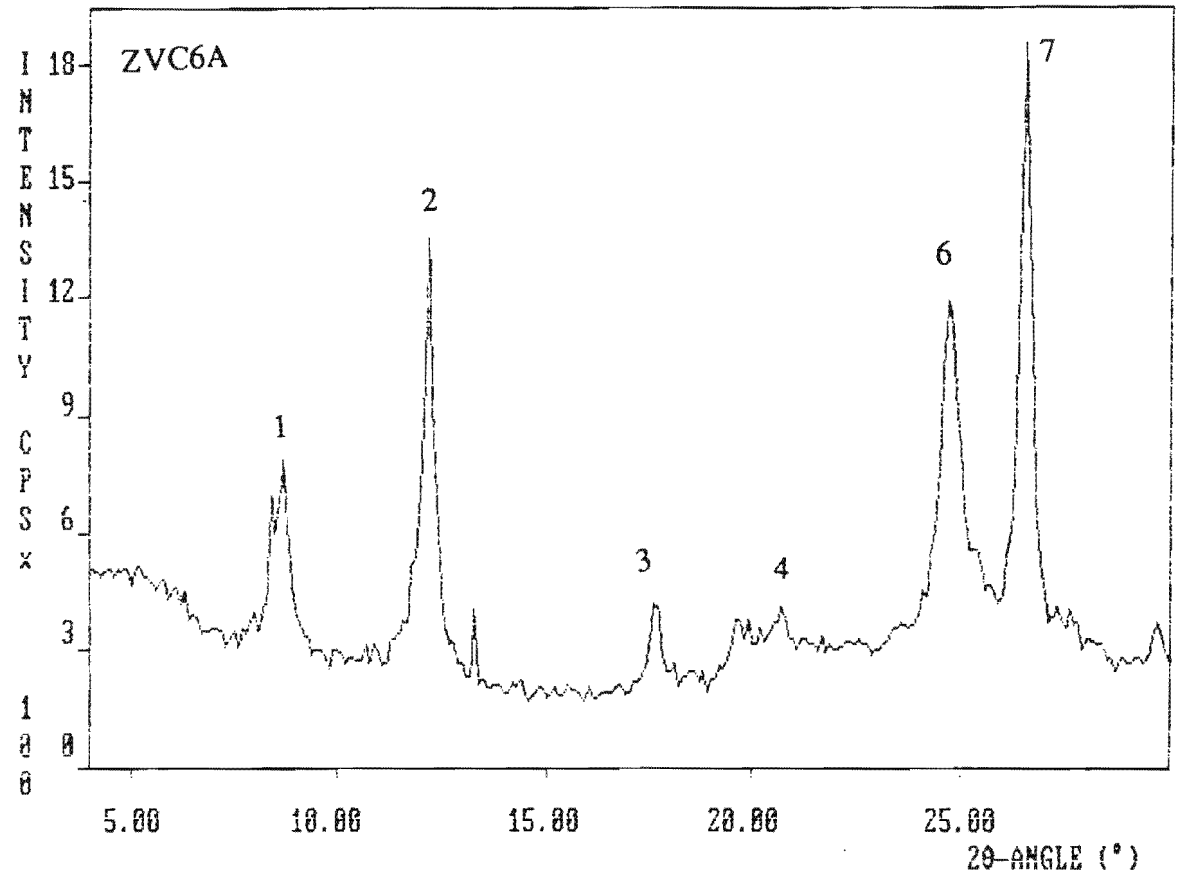

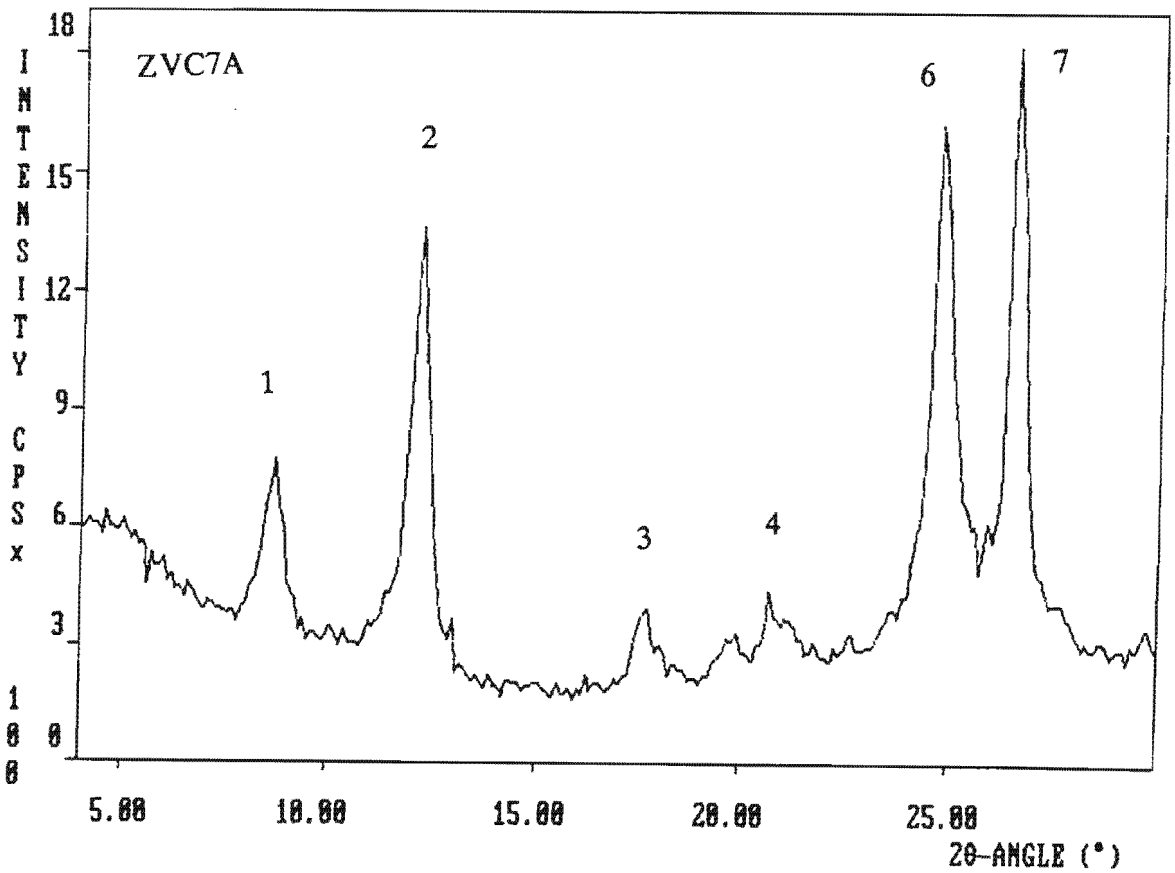

APPENDIX 3

Appendix 3a
Sorption of Pb by ZVC8A

Name	Eq pH	Pb added (ppm)	Eq.Pb(aq)ppm	Eq. Pb(aq) Pb(mmol/l)*100	Pb sorbed Pb(mmol/kgsed)	Kd	Eq. Zn(aq)ppm	Eq. Zn(aq) Zn(mmol/l)*100
zv6a10pbsaltd.w	7.28	10	0.046	0.0222	0.4809	21.66	0.467	0.7146
zv6a60pbsaltd.w	7.55	60	0.117	0.0565	2.8929	51.23	2.630	4.0245
zv6a300pbsaltd.w	7.33	300	0.042	0.0203	14.4907	714.88	2.160	3.3053
zv6a80pbsaltd.w	7.43	80	0.000	0.0000	3.8647		2.070	3.1678
zv6a100pbsaltd.w	6.86	100	0.011	0.0053	4.8304	909.87	1.900	2.9074
zv6a200pbsaltd.w	7.35	200	0.037	0.0179	9.6600	540.96	2.570	3.9327
zv6a500pbsaltd.w	7.2	500	0.057	0.0275	24.1518	877.94	3.870	5.9220
zv6a50pbsaltd.w.	7.69	50	0.050	0.0241	2.4130	100.00	0.917	1.4032
zv6a400pbsaltd.w	7.23	400	0.054	0.0261	19.3211	741.36	3.520	5.3864
zv6a25pbsaltd.w.	7.32	25	0.045	0.0217	1.2056	55.51	0.375	0.5738
zv6a40pbsaltd.w	7.88	40	0.026	0.0125	1.9311	153.89	0.348	0.5325
zv6a80pbsaltd.w	7.36	80	0.000	0.0000	2.8966		0.300	0.4591

Appendix 3b
Sorption of Pb by ZVC7

Name	Eq. pH	Pb added (ppm)	Eq. Pb(ppm)	Eq.Pb(aq) Pb(mmol/l)*100	Pb sorbed Pb(mmol/kgsed)	Kd	Eq.Zn(aq)ppm	Eq.Zn(aq) Zn(mmol/l)*100
zv710pbsaltd.w	7.74	10	0.009	0.0043	0.4822	1110.11	0.069	0.1056
zv750pbsaltd.w.	7.79	50	0.000	0.0000	2.4131		0.058	0.0888
zv7300pbsaltd.w	7.4	300	0.000	0.0000	14.4788		0.149	0.2280
zv740pbsaltd.w	7.25	40	0.000	0.0000	1.9305		0.736	1.1262
zv720pbsaltd.w	8.23	20	0.000	0.0000	0.9653		0.035	0.0538
zv7100pbsaltd.w.	7.92	100	0.000	0.0000	4.8253		0.001	0.0015
zv7200pbsaltd.w.	7.75	200	0.000	0.0000	9.6525		0.001	0.0015
zv780pbsaltd.w	7.75	80	0.000	0.0000	3.8610		0.020	0.0306
zv725pbsaltd.w	7.72	25	0.014	0.0068	1.2059	1784.71	0.017	0.0260
zv7400pbsaltd.w	8.12	400	0.057	0.0275	19.3023	7016.54	0.019	0.0291
zv7500pbsaltd.w.	7.5	500	0.144	0.0695	24.1243	3471.22	0.152	0.2326
zv760pbsaltd.w	7.96	60	0.000	0.0000	2.8958		0.180	0.2754

Appendix 3c
Zn adsorption by ZVC7

Name	Eq. pH	Zn added (ppm)	Eq. Zn(ppm)	Eq. Zn(aq) Zn(mmol/l)*100	Zn sorbed Zn(mmol/kgsed)	Kd
zv750znsaltd.w	7.86	50	0.152	0.2325	7.6232	3279.47
zv740znsaltd.w	7.73	40	0.342	0.5230	6.0648	1159.59
zv780znsaltd.w.	7.66	80	0.496	0.7585	12.1584	1602.90
zv7200znsaltd.w	7.62	200	2.700	4.1291	30.1728	730.74
zv720znsaltd.w	8.11	20	0.362	0.5536	3.0032	542.49
zv730znsaltd.w	8.01	30	0.633	0.9680	4.4911	463.93
zv7100znsaltd.w	7.97	100	0.408	0.6239	15.2305	2440.96
zv7500znsaltd.w	7.29	500	28.200	43.1259	72.1517	167.30
zv760znsaltd.w	7.64	60	0.311	0.4758	9.1282	1919.26
zv7400znsaltd.w	6.67	400	22.400	34.2580	57.7458	168.57

Appendix 3d
Zn sorption by ZVC8A

Name	Eq. pH	Zn added (ppm)	Eq. Zn(ppm)	Eq.Zn(aq) Zn(mmol/l)*100	Zn sorbed Zn(mmol/kgsed)	Kd
zv6a100znsaltd.w	7.58	100	7.460	11.4085	14.1520	124.05
zv6a400znsaltd.w	7.11	400	40.200	61.4773	55.0237	89.50
zv6a60znsaltd.w	7.39	60	4.280	6.5453	8.5212	130.19
zv6a500znsaltd.w	7.33	500	62.400	95.4274	66.9215	70.13
zv6a20znsaltd.w	7.44	20	1.080	1.6516	2.8934	175.19
zv6a80znsaltd.w	8	80	5.530	8.4570	11.3886	134.67
zv6a300znsaltd.w	7.33	300	25.700	39.3026	41.9463	106.73
zv6a200znsaltd.w	7.55	200	15.100	23.0922	28.2765	122.45

APPENDIX 4

Appendix 4a
Pb desorption from ZVC7

Name	Eq pH	Eq Pb(aq)ppm	Eq Pb Pb(mmol/l)*100	Pb(mmol/kg)	Eq Zn(aq)ppm
zv780pbd wdeaex	7.73	0.177	0.0854	3.861	0.028
zv7200pbd wdeaex	7.91	0.112	0.0541	9.653	0.019
zv7400pbd wdeaex	7.84	0.356	0.1726	19.302	0.015
zv7100pbd wdeaex	8.09	0.164	0.0866	4.663	0.017
zv720pbd wdeaex	8.17	0.000	0.0000	0.965	0.043
zv725pbd wdeaex	8.19	0.025	0.0121	1.206	0.024
zv7500pbd wdeaex	7.9	0.107	0.0518	24.124	0.000
zv750pbd wdeaex	8.16	0.150	0.0724	2.413	0.032
zv780pbd wdeaex	8.37	0.000	0.0000	2.896	0.056
zv7300pbd wdeaex	8.48	0.042	0.0203	14.479	0.023
zv710pbd wdeaex	8.19	0.050	0.0241	0.482	0.190
zv740pbd wdeaex	8.07	0.025	0.0121	1.931	1.280

Appendix 4b
Pb desorption from ZVC8A

Name	Eq pH	Eq. Pb(aq)ppm	Pb (mmol/kg)	Eq Zn(aq)ppm	Eq Zn Zn(mmol/l)*100
zv8a25pbd wdeaex	7.38	0.000	1.206	0.875	1.3389
zv8a50pbd wdeaex	8.17	0.000	2.899	0.784	1.1997
zv8a200pbd wdeaex	7.31	0.000	9.660	1.420	2.1729
zv8a10pbd wdeaex	7.18	0.000	0.481	0.370	0.5662
zv8a100pbd wdeaex	7.26	0.000	4.830		0.0000
zv8a40pbd wdeaex	8.23	0.035	1.931	0.074	0.1132
zv8a50pbd wdeaex	7.22	0.000	2.413	1.470	2.2494
zv8a500pbd wdeaex	7.09	0.000	24.152	2.970	4.5448
zv8a400pbd wdeaex	8.06	0.000	19.321	1.190	1.8210

Appendix 4c
Zn desorption from ZVC7

Name	Eq pH	Eq Pb(aq)ppm	Zn Sorbed (ppm)	Zn sorbed Zn(mmol/kg)	Eq Zn(aq)ppm
zv7400znv wdeaex	8.42	0.000	377.800	57.781	1.9500
zv7100znv wdeaex	8.15	0.000	99.592	15.240	0.9950
zv7300znv wdeaex	8.41	0.004			0.7070
zv780znv wdeaex	8.55	0.000	59.689	9.134	0.0750
zv7500znv wdeaex	8.01	0.000	471.800	72.186	8.6500
zv740znv wdeaex	8.42	0.000	49.858	7.599	0.1770
zv730znv wdeaex	8.53	0.000	29.367	4.494	0.0380
zv720znv wdeaex	8.44	0.007	19.638	3.005	0.3880
zv750znv wdeaex	8.54	0.000	49.848	7.628	0.3800
zv7200znv wdeaex	8.4	0.000	197.300	30.191	0.5620

Appendix 4d
Zn desorption from ZVC8A

Name	Eq pH	Eq Pb(aq)ppm	Zn sorbed (ppm)	Zn sorbed Zn(mmol/kg)	Eq Zn(aq)ppm
zv8a40znv wdeaex	8.09	0.000	38.99	5.966	2.060
zv8a30znv wdeaex	8.15	0.000	28.92	4.425	20.000
zv8a100znv wdeaex	7.95	0.000	92.54	14.161	17.800
zv8a200znv wdeaex	7.36	0.000	184.9	28.294	10.300
zv8a300znv wdeaex	7.85	0.000	274.3	41.974	9.790
zv8a500znv wdeaex	7.73	0.000	437.8	66.963	22.400
zv8a20znv wdeaex	7.85	0.000	18.99	2.906	1.880
zv8a80znv wdeaex	7.87	0.000	74.47	11.396	2.810
zv8a100znv wdeaex	8.18	0.000	92.54	14.161	5.060
zv8a400znv wdeaex	7.4	0.010	359.8	55.057	25.800
zv8a50znv wdeaex	7.75	0.000		0.000	3.130
zv8a80znv wdeaex	7.98	0.000	56.72	8.526	2.810

APPENDIX 5

Appendix 5a

The effect of salinity on adsorption

				Zn sorbed		Eq Zn(aq)			Pb sorbed		
Name	Eq pH	NaCl (g/l)	Zn added (ppm)	Zn sorbed (pp	Zn (mmol/kg)	Eq Zn(aq)ppm	Zn(mmol/l)*100	Pb added ppm	Pb sorbed (ppm)	Pb(mmol/kg)	Eq Pb(aq)ppm
zv6a100zn12gnacl	7 28	24	100	85 50	13 0834	14 500	22 1682	0			0 000
zv6a100zn8gnacl	7 83	10	100	91 23	14 2063	8 770	10 3598	0			0 008
zv6a100zn6gnacl	7 56	18	100	90 44	13 8383	8 560	14 8268	0			0 020
zv6a100zn4gnacl	7 58	8	100	93 79	14 3520	6 210	8 5027	0			0 018
zv6a100zn10gnacl	7 14	20	100	87 40	13 3741	12 800	18 2808	0			0 000
zv6a100zn8gnacl	7 41	12	100	82 38	14 1362	8 320	14 2817	0			0 018
zv6a100zn2gnacl	8 06	4	100	86 80	13 7567	10 100	15 4562	0			0 000
zv6a100zn3gnacl	7 56	6	100	93 40	14 2823	6 600	10 0995	0			0 038
zv6a100zn1gnacl	7 3	2	100	86 40	13 5272	11 600	17 7508	0			0 000
zv6a100zn14gnacl	7 23	28	100	84 90	12 8783	15 200	23 2584	0			0 000
zv6a100pb2.5gnacl	7 84	5	0			0 137	0 2098	100	100 000	4 8263	0 000
zv6a100pb1.5gnacl	7 85	3	0			0 328	0 4998	100	99 980	4 8253	0 030
zv6a100pb10gnacl	7 75	20	0			0 492	0 7528	100	99 952	4 8238	0 048
zv6a100pb7gnacl	7 58	14	0			0 267	0 4088	100	99 998	4 8261	0 004
zv6a100pb12gnacl	7 8	24	0			2 450	3 7480	100	99 863	4 8248	0 037
zv6a100pb1gnacl	7 87	2	0			0 095	0 1454	100	99 865	4 8256	0 015
zv6apb1005gnacl	7 87	10	0			0 215	0 3290	100	99 995	4 8260	0 005
zv6a100pb14gnacl	7 28	28	0			2 420	3 7031	100	99 833	4 8230	0 067
zv6apb1003gnacl	7 87	4	0			0 448	0 8625	100	100 000	4 8263	0 000
zv6apb1000 5gnacl	7 88	1	0			0 344	0 5264	100	100 000	4 8263	0 000

Appendix 5b

Salinity induced desorption

Name	Eq pH	NaCl(g/l)	Eq Zn(aq)ppm	Eq Pb(aq)ppm
desz12gnacl	7 25	24	0 134	0 000
desz10gnacl	7 18	20	0 575	0 000
desz8gnacl	7 74	16	0 033	0 000
desz6gnacl	7 28	16	0 043	0 000
desz5gnacl	7 27	10	0 141	0 000
desz3gnacl	7 56	6	0 202	0 000
desz14gnacle w	7 13	28	0 115	0 000

APPENDIX 6

Appendix 6a

Acidity dependent desorption using dilute water acified with HCl

Sample No	Eq pH	Pb(aq) ppm	Zn(aq) ppm	Zn (aq) Zn(mmol/l)*100	Eq pH
1	7.48	0.000	8.640	12.8151	7.71
2	7.08	0.000	10.200	15.8063	7.80
3	6.71	0.000	14.400	22.0352	7.67
4	6.46	0.000	16.800	25.4017	7.67
5	6.24	0.000	18.800	28.8923	7.63
6	6.00	0.000	16.200	24.7886	7.66
7	5.73	0.000	21.100	32.2877	7.46
8	5.58	0.000	18.800	28.7982	7.28
9	5.23	0.000	17.600	26.6316	7.33
10	3.82	0.000	16.100	26.2272	7.70
11	4.28	0.000	21.600	33.3586	7.74
12	3.80	0.000	23.500	35.9602	7.23

Appendix 6b

pH dependent desorption using nitric acid

Sample No	Eq pH	Pb(aq)ppm	Zn(aq)ppm	Zn (aq) Zn(mmol/l)*100	Conc HNO3(M)
9	2.80	0.000	0.242	0.3703	0.150
5	6.88	0.000	18.400	28.1561	0.050
6	6.75	0.015	37.800	57.9954	0.060
7	5.10	0.001	75.400	115.3787	0.075
8	4.66	0.000	85.400	130.6609	0.080
1	7.28	0.081	4.620	7.0696	0.010
2	7.32	0.018	8.070	8.2584	0.020
3	7.91	0.016	6.710	10.2678	0.030
4	7.08	0.032	13.800	21.1171	0.040

Appendix 7. Statistical parameters calculated using Statgraphics, for the entire data set listed in Appendix 1.

Variable	Pb	Zn	Cu	% Org C
Sample Size	79	79	79	31
Average	189.2	991.9	51.87	3.24
Median	160	795.5	49	3.59
Mode	202	103	18	0.54
Geo. mean	136.5	543.0	40.4	2.69
variance	26143	$1*10^6$	1160.4	3.00
std. dev.	161.7	1002.1	34.1	1.73
std. err.	18.2	112.7	3.8	0.31
Minimum	7.3	10	3.3	0.54
Maximum	990	5183	200	7.72
Range	982.7	5173	196.7	7.18
Lower quart.	89	211	21	1.76
Upper qaurt.	232	1237.1	71	4.13
interq. range	143	1026.1	50	2.37
skewness	2.83	1.76	1.22	0.39
std. skewness	10.28	6.40	4.44	0.88
kurtosis	11.55	3.73	3.24	0.22
std. kurt.	20.96	6.77	5.88	0.25
coeff. var.	85.45	101.04	65.67	53.41
sum	14947	78356.2	4097.9	100.5

APPENDIX 8.

Statistical parameters calculated using Statgraphics, for surface samples only, listed in Appendix 1.

Variable	Pb	Zn	Cu
Sample Size	67	67	67
Average	167.3	1011.6	54.4
Median	160	839.4	51
Mode	41	816	15
Geo. mean	129.9	604.1	43.1
variance	10065	781739	1187.2
std. dev.	100.3	884.2	34.5
std. err.	12.3	108.0	4.2
Minimum	16	30	8.6
Maximum	472	3830	200
Range	456	3800	191.4
Lower quart.	97	270	24
Upper qaurt.	224	1298.4	71
interq. range	127	1028.4	47
skewness	0.58	1.21	1.22
std. skewness	1.95	4.04	4.07
kurtosis	0.44	1.20	3.48
std. kurt.	0.74	2.01	5.82
coeff. var.	59.96	87.40	63.34
sum	11211.6	67780.2	3644.8

APPENDIX 9.

Spearman rank correlation coefficients calculated using Statgraphics to determine the degree of association of Pb, Cu, Zn and organic carbon in the sediments. Sample size = 31.

	Pb	Cu	Zn
Org C	0.72	0.72	0.71
Zn	0.91	0.93	
Cu	0.97		

Appendix 10a. Calculated Z statistic using the Mann-whitney U test to determine the degree of non-equivalence of the industrial and residential sediment samples with regards to Pb, Zn and Cu.

```
Sample 1: SEDRESPA.Pbppm

Sample 2: SEDINDPA.Pbppm

Test: Unpaired

Average rank of first group = 17.3158 based on 19 values.
Average rank of second group = 22.55 based on 20 values.
Large sample test statistic Z = 1.41914
Two-tailed probability of equaling or exceeding Z = 0.155857

NOTE:  39 total observations.
```

```
Sample 1: SEDRESPA.Znppm

Sample 2: SEDINDPA.Znppm

Test: Unpaired

Average rank of first group = 16.9211 based on 19 values.
Average rank of second group = 22.925 based on 20 values.
Large sample test statistic Z = 1.62974
Two-tailed probability of equaling or exceeding Z = 0.103156

NOTE:  39 total observations.
```

```
Sample 1: SEDRESPA.Cuppm

Sample 2: SEDINDPA.Cuppm

Test: Unpaired

Average rank of first group = 17.3158 based on 19 values.
Average rank of second group = 22.55 based on 20 values.
Large sample test statistic Z = 1.41914
Two-tailed probability of equaling or exceeding Z = 0.155857

NOTE:  39 total observations.
```

Appendix 10b. Calculated Z statistic using the Mann-whitney U test to determine the degree of non-equivalence of the sediment samples from the northern and southern pans with regards to Pb, Zn and Cu.

```
Sample 1: SEDPANA.Pbppm

Sample 2: SEDPANB.Pbppm

Test: Unpaired

Average rank of first group = 30.8333 based on 42 values.
Average rank of second group = 18.8462 based on 13 values.
Large sample test statistic Z = -2.34766
Two-tailed probability of equaling or exceeding Z = 0.0188919

NOTE:  55 total observations.
```

```
Sample 1: SEDPANA.Znppm

Sample 2: SEDPANB.Znppm

Test: Unpaired

Average rank of first group = 33 based on 42 values.
Average rank of second group = 11.8462 based on 13 values.
Large sample test statistic Z = -4.15035
Two-tailed probability of equaling or exceeding Z = 3.32166E-5

NOTE:  55 total observations.
```

```
Sample 1: SEDPANA.Cuppm

Sample 2: SEDPANB.Cuppm

Test: Unpaired

Average rank of first group = 30.8571 based on 42 values.
Average rank of second group = 18.7692 based on 13 values.
Large sample test statistic Z = -2.36772
Two-tailed probability of equaling or exceeding Z = 0.0178979

NOTE:  55 total observations.
```

APPENDIX 11

Spearman rank correlation coefficients calculated using Statgraphics to determine the degree of dissolved Pb, Cd, Zn, Fe and organic carbon in the vlei water.

Sample size = 64

	Cd	Fe	Zn	Pb
DOC	0.26	0.31	-0.31	-0.11
Pb	0.04	0.16	0.58	
Zn	-0.06	0.21		
Fe	0.15			

APPENDIX 12

Solubilty of lead carbonate

Name PbNO3	pH	Eq Pb(ppm)	Eq. Pb Pb(mmol/l)*100	Pb added(ppm)	Pb added Pb(mmol/l)*100	Pb removed Pb(mmol/l)*100
pbno3ex30pb	7.97	7.28	3.5135	30	14.4788	10.9653
pbno3ex100pb	7.7	3.34	1.6120	100	48.2625	46.6506
pbno3ex50pb	8.09	5.81	2.8041	50	24.1313	21.3272
pbno3ex10pb	8	3.71	1.7905	10	4.8263	3.0357
pbno3ex200pb	7.75	4.78	2.3069	200	96.5251	94.2181
pbno3ex60pb	7.81	6.69	3.2288	60	28.9575	25.7288
pbno3ex20pb	7.89	1.90	0.9170	20	9.6525	8.7355
pbno3ex400pb	7.71	32.28	15.5792	400	193.0502	177.4710
pbno3ex500pb	5.97	74.00	35.7143	500	241.3127	205.5985
pbno3ex40pb	7.84	2.70	1.3031	40	19.3050	18.0019
pbno3ex300pb	6.79	16.60	8.0116	300	144.7876	136.7761
pbno3ex450pb	6.32	52.38	25.2799	450	217.1815	191.9015

APPENDIX 13

Speciation of Pb and Zn in selected Zoar Vlei sediments. These results are taken from Board (1993) and Farmer (1993), and are determined by the sequential extraction technique proposed by Tessier *et al.* (1979). Exchang. phases = easily exchangeable metal; carb. phases = metal bound to carbonate phases; oxide phases = metal bound to oxide phases; org matt. + sulphide phases = metal associated with organic matter and sulphides; tot. ppm = total concentration of metal in ppm.

		exchan. phases (%)	carb. phases (%)	oxide phases (%)	org matt. + sulphide phases (%)	inert metal (%)	tot. ppm
Pb	A2S1	3.80	8.54	41.76	8.54	37.36	163
	A3S1	1.59	1.59	40.14	45.95	10.73	587
	B2S1	3.73	2.66	37.27	42.60	13.74	291
	B3S1	4.65	3.10	40.27	31.75	20.23	400
	B11S1	2.77	5.54	44.35	26.33	21.01	224
	B16S1	2.68	4.28	46.02	2.14	44.88	290
	D4S1	4.77	2.38	50.83	31.77	10.25	195
Zn	A2S1	0.69	27.34	61.41	4.15	6.41	1451
	A3S1	8.87	13.21	62.62	11.90	3.40	2450
	B2bS1	2.32	9.30	69.70	13.37	5.31	1901
	B3S1	15.47	9.62	53.99	16.66	4.26	2885
	B11S1	0.49	14.75	67.97	11.28	5.51	1072
	B16S1	1.80	4.15	73.58	13.08	7.39	948
	D4S1	0.57	1.41	76.79	13.54	7.69	767